ChemPubSoc Europe

DOI: 10.1002/chem.201501334

CHEMISTRY A European Journal Full Paper

Enzymes

Recognition of Artificial Nucleobases by *E. coli* Purine Nucleoside Phosphorylase versus its Ser90Ala Mutant in the Synthesis of Base-Modified Nucleosides

Ilja V. Fateev,[a] Maria I. Kharitonova,[a] Konstantin V. Antonov,[a] Irina D. Konstantinova,[a] Vasily N. Stepanenko,[a] Roman S. Esipov,[a] Frank Seela,[b] Kartik W. Temburnikar,[c] Katherine L. Seley-Radtke,[c] Vladimir A. Stepchenko,[d] Yuri A. Sokolov,[d] Anatoly I. Miroshnikov,[a] and Igor A. Mikhailopulo*[d]

Abstract: A wide range of natural purine analogues was used as probe to assess the mechanism of recognition by the wild-type (WT) *E. coli* purine nucleoside phosphorylase (PNP) versus its Ser90Ala mutant. The results were analyzed from viewpoint of the role of the Ser90 residue and the structural features of the bases. It was found that the Ser90 residue of the PNP 1) plays an important role in the binding and activation of 8-aza-7-deazapurines in the synthesis of their nucleosides, 2) participates in the binding of α-D-pentofuranose-1-phosphates at the catalytic site of the PNP, and 3) catalyzes the dephosphorylation of intermediary formed 2-deoxy-α-D-ribofuranose-1-phosphate in the trans-2-deoxyribosylation reaction. 5-Aza-7-deazaguanine manifested excellent substrate activity for both enzymes, 8-amino-7-thiaguanine and 2-aminobenzothiazole showed no substrate activity for both enzymes. On the contrary, the 2-amino derivatives of benzimidazole and benzoxazole are substrates and are converted into the N1- and unusual N2-glycosides, respectively. 9-Deaza-5-iodoxanthine showed moderate inhibitory activity of the WT *E. coli* PNP, whereas 9-deazaxanthine and its 2′-deoxyriboside are weak inhibitors.

Introduction

Recently, we have disclosed satisfactory substrate properties for a number of representatives of the pyrazolo[3,4-*d*]pyrimidine (8-aza-7-deazapurine) scaffolds **1**–**4** for the recombinant *E. coli* purine nucleoside phosphorylase (PNP) (Figure 1).[1] The most surprising finding was the observation of substrate activity of 2-amino-8-aza-6-chloro-7-deazapurine (**4**) that was enzymatically converted into its 2′-deoxyriboside **4a** as the main product (40–55% according to HPLC) and isolated from the reaction mixture in a 25% yield. A careful analysis of the published crystallographic data of the catalytic site of the *E. coli* PNP allowed us to hypothesize that the key role of the side chain of Ser90-OγH involves the initial recognition followed by the formation of the glycosyl bond in the synthesis of 8-aza-7-deazapurine nucleosides.[1] In that regard, the close proximity of the Ser90 hydroxyl group to the imidazole ring of the adenine bound at the catalytic site of the *E. coli* PNP containing also α-D-ribofuranose-1-phosphate (Rib-1P)[2,3] was a clue for such suggestion. Note that this proximity may be responsible for the absence of substrate activity of the C8-substituted purines (except for 8-aminoadenine, see below) for the *E. coli* PNP. Ab initio analyses of the possible tautomeric structures of 8-aza-7-deazapurine in a complex with the Ser90 hydroxyl group showed that the spatial arrangements of the N9-amino sp^3-hybridized (=N8-N9(H)-C4, purine numbering throughout this paper) tautomer and the sp^2-hybridized N9-imino (-(H)N8-N9=C4) tautomer are compatible with the suggested equilibrium implying the nucleophilic attack of the N9-imino nitrogen atom on the electrophilic C1 atom of Rib-1P in the synthesis reaction.[1,4]

Remarkably, a PNP preparation from human erythrocytes was shown to be capable to catalyze the ribosylation of allopurinol (**3**) that was converted into 8-aza-7-deaza-9-(β-D-ribofuranosyl)-purine-6-one (allopurinol ribosides, Allo-Rib) by using diverse ribosyl donors (i.e., uridine, inosine, xanthosine, or Rib-1P) and the biocatalysts.[5,6] The mechanism of the

[a] *Dr. I. V. Fateev, M. I. Kharitonova, K. V. Antonov, Dr. I. D. Konstantinova, Dr. V. N. Stepanenko, Dr. R. S. Esipov, Prof. A. I. Miroshnikov*
Department of Biotechnology
Shemyakin and Ovchinnikov Institute of Bioorganic Chemistry
RAS, Miklukho-Maklaya 16/10, 117997 GSP
Moscow B-437 (Russian Federation)

[b] *Prof. F. Seela*
Laboratory of Bioorganic Chemistry and Chemical Biology
Center for Nanotechnology
Heisenbergstr. 11, 48149 Münster (Germany)

[c] *Dr. K. W. Temburnikar, Prof. K. L. Seley-Radtke*
University of Maryland, Baltimore County, 1000 Hilltop Circle
Baltimore, Maryland 21250 (USA)

[d] *V. A. Stepchenko, Dr. Y. A. Sokolov, Prof. I. A. Mikhailopulo*
Institute of Bioorganic Chemistry, National Academy of Sciences
220141 Minsk, Acad. Kuprevicha 5/2 (Belarus)
E-mail: imikhailopulo@gmail.com

Supporting information for this article is available on the WWW under http://dx.doi.org/10.1002/chem.201501334.

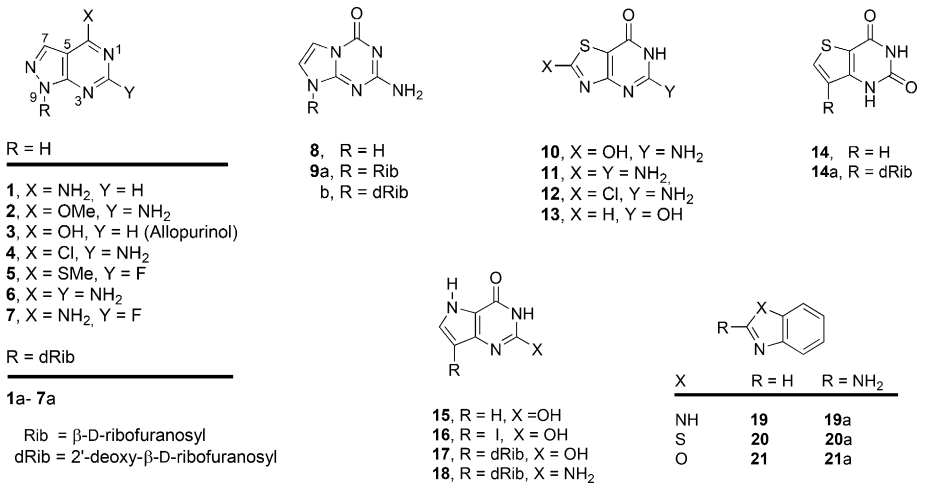

Figure 1. Structures of the 8-aza-7-deazapurines **1**–**7** and their 2′-deoxy-β-D-ribofuranosides **1a**–**7a**, 5-aza-7-deazaguanine (**8**, $^{5A:7DA}$Gua) and its glycosides **9a** and **9b** ($^{5A:7DA}$G and $^{5A:7DA}$dG), the 7-thiapurines **10**–**14**, the 9-deazapurines **15** and **16**, the 2′-deoxy-β-D-ribofuranosides of 9-deazaxanthine (**17**) and -guanine (**18**), as well as 1,3-benzimidazole (BI, **19**), 1,3-benzthiazole (BT, **20**), and 1,3-benzoxazole (BO, **20**) and their respective 2-amino derivatives **19a**–**21a**. Purine numbering is used throughout the text.

heterocyclic substrate binding and its activation was not investigated.[6] However, it is noteworthy that an analysis of the ternary complex of the *E. coli* PNP, sulfate or phosphate, and formycin B (Figure 2), which is a strong inhibitor of the *E. coli*

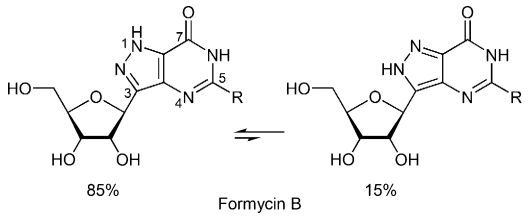

Figure 2. Main tautomers of formycin B.

PNP,[7a,b] led the authors to conclude that the N2-H tautomer of formycin B may form a hydrogen bond to the Ser90-(H)Oγ oxygen atom.[7a,8] Notably, based on the crystallographic data, the Ser90 residue of the catalytic site of the *E. coli* PNP was suggested to participate in the binding of inorganic phosphate[2,8–10] and the ribose moiety[8,10] of a purine nucleoside in the phosphorolysis reaction.[2,3,8–11]

It is presently broadly accepted that the β-carboxyl group of the Asp204 residue of the catalytic site of *E. coli* PNP plays an important role in the binding of natural purine nucleosides by means of the protonation of the N7 nitrogen atom followed by activation leading to phosphorolytic scission of the glycosyl bond[2,3] (for recent reviews, see reference [4]). Indeed, the replacement of the Asp204 residue by L-alanine gave rise to the Asp204Ala mutant of *E. coli* PNP, the phosphorolytic activity of which was dramatically reduced.[3,12] There are only few exceptions from this postulate and some of them are exemplified by the very efficient phosphorolysis of N7-methylguanosine (**21a**) and its 2′-deoxy-counterpart **21b** (see below), the positively charged N7 atom of which mimics an enzymatic protonation.[13–15]

Taking into account that *E. coli* PNP catalyzes the reversible phosphorolysis of purine nucleosides, one can expect that the Asp204 side chain makes the main contribution in the binding of the heterocyclic substrate in the synthetic reaction. The Asp204 interacts with the N7 atom and/or substituent at the C6 atom (NH_2, NHR, carbonyl, OR) of the purine base giving rise, in all likelihood, to the proper base positioning at the catalytic site and to an enhancement of the nucleophilic properties of the N9 atom, that is, activation of the substrate.[1] It was, therefore, surprising that a replacement of the N7 atom with a CH group did not abolish the substrate activity of bases **1**–**3** pointing to the rather efficient contribution of the Asp204 βC(=O)O–H···XC6 (X = NH_2, OMe, or carbonyl) interaction in the correct binding and activation of the substrates. However, 2-amino-8-aza-7-deaza-6-chloropurine (**4**) does not contain a N7 atom and moreover contains a chlorine atom at the C6 atom that is unable to take part in the hydrogen bonding and none the less showed satisfactory substrate activity for *E. coli* PNP.

To gain further insight into the role of the Ser90 side chain of the catalytic site of *E. coli* PNP in the recognition of the 8-aza-7-deazapurines **1**–**4** as well as a number of other purine analogues in the synthesis reaction, we 1) prepared the Ser90Ala mutant of the *E. coli* PNP [see the Supporting Information, with the preparation of the wild-type *E. coli* PNP[16]], 2) analyzed kinetic parameters of the transribosylation of hypoxanthine, allopurinol (**3**), and 5-aza-7-deazaguanine (**8**, $^{5A:7DA}$Gua) by using the wild-type (WT) *E. coli* PNP versus the mutant enzyme, 3) investigated the substrate activity of 8-aza-7-deazapurines toward the WT *E. coli* PNP, (iv) tested the substrate properties of a number of challenging purine analogues, that is, the 7-thiaguanines **10**–**14**, the 9-deazapurines **15**–**18**, and 1,3-benzimidazole (**19**), 1,3-benzthiazole (**20**), and 1,3-benzoxazole (**21**), and their 2-amino derivatives **19a**–**21a** towards both enzymes. The results have been analyzed from viewpoint of the electronic structures of the bases and suggested possible modes of substrate recognition aiming at the implication for the enzymatic synthesis of new nucleosides.

It should be emphasized that the motivation of this work is that the *E. coli* PNP is very valuable in biotechnology of modified nucleosides, including a number of antiviral and anticancer drugs.[2–4] Analysis of the biocatalytic potential of this enzyme, as well as an understanding of the mechanism of its functioning are of considerable interest for the design of new substrates and/or inhibitors as well as for the synthesis of new analogues of natural purine nucleosides that are of potential importance for molecular biology and medicine.

Results and Discussion

Substrate specificity of the WT *E. coli* PNP versus that of the Ser90Ala mutant

The transribosylation of hypoxanthine and 8-aza-7-deazahypoxanthine (**3**, allopurinol, Allo) by using uridine and the recombinant *E. coli* uridine phosphorylase (UP)[16] for the in situ generation of intermediary Rib-1P revealed the differences in the reaction rates at the starting phase of the synthesis catalyzed by the WT *E. coli* PNP versus the Ser90Ala mutant (Figure 3). In the presence of the former, the formation of 1) inosine reached approximately 80% in 30 min and after the next 30 min established an equilibrium of hypoxanthine+Rib-1P⇄inosine+inorganic phosphate (Pi) at a base/nucleoside ratio of approximately 2:8 in the reaction mixture and 2) allopurinol riboside (Allo-Rib) proceeded somewhat slower achieving a 95% conversion of allopurinol (**3**) to its N9 riboside after 24 h. Thus, the reversible condensation of Rib-1P and hypoxanthine is displaced to the product formation, whereas the formation of Allo-Rib proceeded irreversibly as it was proven by the experiments with 8-aza-7-deaza-9-(2-deoxy-β-D-ribofuranosyl)-purin-6-one (**3a**, Allo-dRib) and the WT *E. coli* PNP. The Allo-dRib was not phosphorolyzed by *E. coli* PNP and this result is in consent with the earlier data on the crucial importance of the N7 atom of purine nucleosides in an analogous reaction (reviewed in reference [4]).[17,18]

The similar substrate properties of hypoxanthine and allopurinol for the WT *E. coli* PNP indicate a non-critical role of the N7 atom of the heterocyclic substrate in the enzymatic synthesis of nucleosides. As discussed above, two hydrogen bonds between the β-carboxyl group of the Asp204 residue (side chain) and the N7 atom and the C6 carbonyl group[2,11] are responsible for the correct binding/activation of hypoxanthine in the productive complex of the WT *E. coli* PNP. In the case of allopurinol (**3**), the binding and activation are realized by the side chain of Asp204 and the C6=O function as well as by the Ser90–(H)Oγ···H–N8 hydrogen bond that makes a compensation for the loss of the Asp204/N7 hydrogen bond (Figure 3).[1,4]

Replacement of the WT *E. coli* PNP with the mutant enzyme in the synthesis reactions resulted in 1) the reduction of the initial rate of the inosine formation (35% yield of inosine in one hour; an equilibrated mixture with a base/nucleoside ratio of ca. 2:8 after 24 h) and 2) a significant decrease of the rate of the Allo-Rib formation attaining a approximately 20% yield after 48 h. A slight reduction of the rate of the inosine formation without loss of the catalytic efficiency points to a moderate contribution of the Ser90 side chain of the catalytic center of the WT *E. coli* PNP in the binding of hypoxanthine[2,9] and/or Rib-1P[10] in the presence of all the natural factors, responsible for the catalytic efficiency. On the contrary, the Ser90 residue of the WT *E. coli* PNP is of unique importance in the binding and activation of allopurinol as well as other 8-aza-7-deazapurines in the enzymatic synthesis of their nucleosides. It is obvious that a hydrogen bond between Asp204 and the C6 carbonyl function of allopurinol is an important factor in the observed formation of Allo-Rib in the reaction catalyzed by the mutant PNP. Indeed, 2-amino-8-aza-6-chloro-7-deazapurine (**4**) was transformed into its riboside in a yield of less than 1% after 48 h (HPLC) under similar reaction conditions.

Replacement of Ser90 with L-alanine eliminates the possible interactions with hypoxanthine and/or Rib-1P resulting in the retardation of the velocity of the inosine formation catalyzed by the mutant enzyme; however,

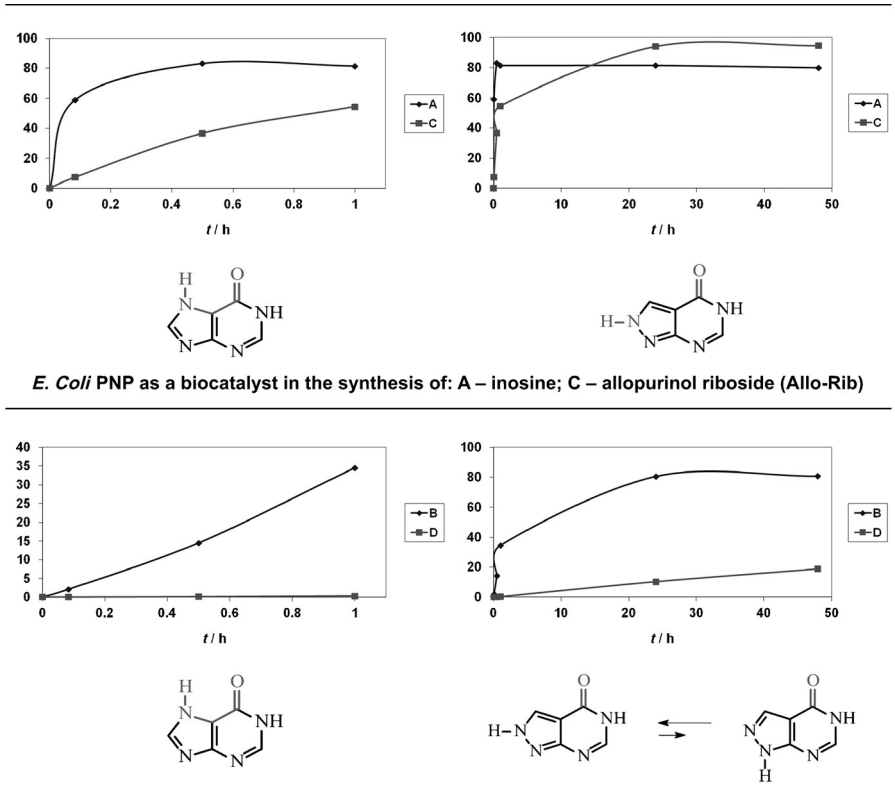

Figure 3. Progress of the synthesis of inosine versus allopurinol riboside (HPLC ratio [%]) by using the WT *E. coli* PNP and the Ser90Ala mutant of the PNP. Reaction conditions: reactions (1.0 mL) were performed in the presence of hypoxanthine or allopurinol (2 mM) and uridine (2 mM) in buffer solution (pH 7.0, 2 mM KH_2PO_4) and the recombinant *E. coli* enzymes (15 μg of the WT *E. coli* PNP or the Ser90Ala mutant and 9 μg of the recombinant *E. coli* UP[16]) at 50 °C for 48 h.

when the equilibrium was reached after 24 h, a similar 2:8 stoichiometric mixture of hypoxanthine/inosine was obtained. On the contrary, in the case of the synthesis of Allo-Rib catalyzed by the WT *E. coli* PNP the main function of the Ser90 residue appears to be the initial binding followed by an activation of allopurinol (**3**) and dramatic loss of efficiency of the product formation by going from the wild type to the mutant enzyme is in harmony with this suggestion.

In order to gain further insight in the mechanism of the glycosyl bond formation, the formation of inosine, Allo-Rib, and 5-aza-7-deazaguanosine (**9a**) (Figure 4) catalyzed by PNP of both

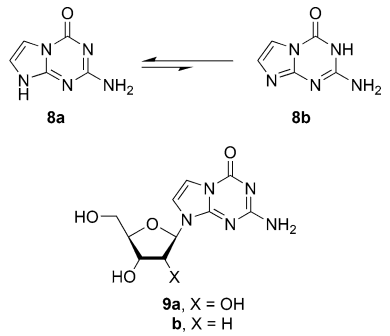

Figure 4. Structures of the tautomers **8a** and **8b** of 5-aza-7-deazaguanine (**8**) and its nucleosides **9**.

types was investigated in detail. The selection of this set of compounds was based on one common structural motif comprising the presence of C6=O carbonyl groups with rather similar electronic structure (Table S1 in the Supporting Information). Thus, hypoxanthine may participate in the formation of two hydrogen bonds with the Asp204 side chain (compare references [2, 11]); allopurinol (**3**) may form a hydrogen bond with Asp204 and the other with the Ser90-OγH hydroxyl group, whereas 5-aza-7-deazaguanine (**8**) has only one possibility to form a hydrogen bond between the C6=O functionality and the Asp204 side chain (Table 1).

First of all, we studied the formation of ribosides and found that inosine is synthesized approximately 30 and 1.9 times faster than Allo-Rib and 5-aza-7-deazaguanosine (**9a**), respectively, catalyzed by the WT *E. coli* PNP (Table 1). As expected, in the case of the mutant *E. coli* PNP, the synthesis of Allo-Rib proceeded with substantially reduced (463 times slower) efficiency as compared with that of inosine, pointing to the importance of the Ser90 residue in this reaction. On the contrary, 5-aza-7-deazaguanosine (**9a**) was synthesized surprisingly 1.8 times faster than inosine. On the other hand, the efficiency of the syntheses of inosine, Allo-Rib, and 5-aza-7-deazaguanosine (**9a**) is decreased by 93, 1438, and 28 times, respectively, in the transition from the wild-type enzyme to the mutant enzyme (Table 1).

Table 1. Rates of the inosine, Allo-Rib, and 5-aza-7-deazaguanosine (**9a**, $^{5A:7DA}$G) formation catalyzed by the WT and Ser90Ala *E. coli* PNPs.[a]

Product of the synthetic reaction	Formation rate [μmol min^{-1} per mg of enzyme]	
	wild-type PNP	Ser90Ala PNP
inosine	69	0.74
allopurinol riboside (Allo-Rib)	2.3	0.0016
5-aza-7-deazaguanosine (**9a**; $^{5A:7DA}$G)	37	1.3

[a] Reaction conditions: reaction mixtures (1 mL) contained uridine (4 μmol), hypoxanthine, allopurinol, or 5-aza-7-deazaguanine (2 μmol), and potassium phosphate (20 μmol). The reactions were initiated by addition of the recombinant *E. coli* enzymes UP (6.6 μg) and WT PNP (from 0.34 to 0.68 μg) or the Ser90Ala mutant PNP (from 2.4 to 18 μg). The reactions were performed at room temperature and pH 7.0 and the progress of the reaction was monitored by HPLC. Each reaction was conducted in triplicate and average values are given.

A significant reduction in the catalytic power of the mutant enzyme versus that of the WT *E. coli* PNP in the synthesis of allopurinol riboside agrees with our hypothesis[1] (see above). However, the reason for the differences in the drop of the substrate activity of hypoxanthine (93 times) versus that of 5-aza-7-deazaguanine (28 times) is not obvious. We hypothesize that the characteristics of the electronic structures of hypoxanthine and $^{5A:7DA}$Gua (**8**) may provide a clue to the understanding of the observed differences in the velocity of the enzymatic glycosylation. With this aim in view, we analyzed the electronic properties of the compounds under study by the ab initio method (restricted Polak–Ribiere (RPR) method by using basis set of the 6-31G** level; the files of the PM3 geometry optimization were used as starting approximation for the ab initio calculations; HyperChem 8.1 (Hypercube, Inc., 1115 NW 4th St. Gainesville, FL 32601, USA; www.hyper.com) and compared them to structurally similar natural substrates (see the Supporting Information, Table S1).

According to the quantum chemical parameters, hypoxanthine populates in an approximately 1:1 mixture of the sp^3-hybridized N9 and the sp^2-hybridized tautomers, whereas the equilibrium of allopurinol is imperceptibly displaced to the sp^3-hybridized N9 structure. Remarkably, the partial negative charge of the sp^2-hybridized N9 tautomer of hypoxanthine ($-$0.563 e) is higher (the absolute value!) compared with that of allopurinol ($-$0.385 e) implying the higher nucleophilicity of the former. These data are in consent with the observed higher reactivity of hypoxanthine in the transribosylation reaction catalyzed by the WT *E. coli* PNP (see above). The sp^3-hybridized N9 (**8a**)$\rightleftarrows$sp^2-hybridized (**8b**) equilibrium of 5-aza-7-deazaguanine (**8**) is slightly biased toward the former structure (Figure 4). The partial negative charges of the sp^2-hybridized N9 atoms of hypoxanthine, allopurinol, and the guanine analogue **8b** are in satisfactory agreement with the observed reactivity of these bases toward both PNPs.

Comparative kinetics of the reactions catalyzed by the wild-type *E. coli* PNP and its mutant

The aforementioned considerations prompted us to study the kinetics of the synthesis of inosine, Allo-Rib, and 5-aza-7-deazaguanosine (**9a**) by the condensation of the corresponding bases with α-D-ribofuranose-1-phosphate (Rib-1P) catalyzed by the WT *E. coli* PNP and the mutant enzyme (Table 2) (for details, see the Experimental Section).

Table 2. Kinetic parameters for the synthesis of the ribosides of hypoxanthine, allopurinol, and 5-aza-7-deazaguanine (**8**) and for the phosphorolysis of inosine catalyzed by the WT *E. coli* PNP versus those catalyzed by the Ser90Ala mutant PNP (for details, see the Experimental Section).

Substrate	K_m [mM]	V_{max} [μmol min^{-1} mg^{-1}]	k_{cat} [s^{-1}]	Relative catalytic constant[a]
wild-type *E. coli* PNP				
hypoxanthine	(0.041 ± 0.006)	(59 ± 12)	(153 ± 31)	57
allopurinol (**3**)	(0.16 ± 0.02)	(1.0 ± 0.1)	(2.7 ± 0.2)	1
5-aza-7-deaza-guanine (**8**)	(0.15 ± 0.01)	(34 ± 6)	(90 ± 15)	33
inosine	(0.052 ± 0.008)	(25 ± 2)	(66 ± 5)	5.5
Ser90Ala mutant				
hypoxanthine	(20 ± 3)	(5.3 ± 0.4)	(14 ± 1)	4000
allopurinol (**3**)	(0.17 ± 0.01)	(0.0014 ± 0.0003)	(0.0035 ± 0.0009)	1
5-aza-7-deaza-guanine (**8**)	(0.14 ± 0.02)	(0.10 ± 0.03)	(0.26 ± 0.09)	74
inosine	(9.2 ± 1.2)	(4.6 ± 1.6)	(12.0 ± 4.0)	1

[a] The lowest value of the catalytic constant k_{cat} for the WT and the mutant *E. coli* enzyme was taken for one (1) in the relevant calculations.

Binding of hypoxanthine at the catalytic site of the WT *E. coli* PNP is realized mainly through the hydrogen bonding between the Asp204 side chain and the N7 and the C6 carbonyl group of the base (see references [2,11]). Replacement of Ser90 with L-alanine does not disturb this interaction; however, essential loss of the hypoxanthine affinity (increase of the Michaelis–Menten constant K_m value 490 times) is likely associated with the Ser90/base interaction, the origin of which is unknown (see, e.g., references [2,9]). The decrease of the maximum initial velocity (V_{max}) and the catalytic constant (turnover number, k_{cat}) both by approximately one order of magnitude are likely related to the absence of the side chain of Ser90/Rib-1P interaction (see, references [3,10]).

The affinity of allopurinol and 5-aza-7-deazaguanine for the WT *E. coli* PNP is only four times lower compared to hypoxanthine. The K_m values for the ribosylation of both analogues are very similar and remain practically unchanged at transition from the wild-type enzyme to a mutant enzyme. On the whole, the changes of the K_m values in experiments with the wild-type and mutant enzymes, as well as in the transition from the wild-type to the mutant enzyme can be explained by the interplay of different factors, such as the residual charges of the C6 carbonyl groups of all the studied bases, the efficiency of the C6=O/Asp204 side chain, and the side chain of Ser90/bases interactions, herewith the contribution of the latter interaction on the K_m values for hypoxanthine is more essential compared to the purine analogues.

The breakdown of the substrate–WT *E. coli* PNP complex and the release of the ribosides of the analogues proceed approximately 60 times slower in the case of Allo-Rib and about 1.7 times slower in the case of 5-aza-7-deazaguanosine (**9a**) versus that of inosine. It can be assumed that the Ser90–OγH···N8 hydrogen bond reduces the release rate of the Allo-Rib molecule formed from the catalytic site of the enzyme, which leads to the lowest V_{max} and k_{cat} values of the ribosylation reaction in comparison with the same kinetic parameters for two other nucleoside syntheses in which such a hydrogen bond is absent.

In the transition from the wild-type *E. coli* PNP to a mutant enzyme, the catalytic constant k_{cat} of the ribosylation of hypoxanthine, allopurinol, and 5-aza-7-deazaguanine (**8**) decreased by approximately 10, 770, and 346 times, respectively. As expected, among the compounds studied, allopurinol showed the lowest substrate efficiency. These data undoubtedly point to an important role of the Ser90–OγH···N8(9) interaction of allopurinol in the synthesis of its riboside.

The similarity of the kinetic parameters of two analogues has no straightforward explanation owing to, first of all, unique substrate properties of 5-aza-7-deazaguanine (**8**). Indeed, it was shown that 5-aza-7-deazaguanine (**8**) is a substrate of mammalian[4a,19] and bacterial[20] PNPs, despite the known differences in the binding and activation of natural substrates, namely, 1) Asn243 of the human PNP (hPNP) participates in the substrate binding instead of Asp204 of the WT *E. coli* PNP; note that the C6=O···H–N(H)–Cβ(=O)–Asn243 hydrogen bond is weaker than that of C6=O···HO–C(=O)–R of Asp204 owing to a lower "donor strength" of the amide group of Asn243,[21] and nonetheless the glycosyl bond formation takes place; 2) hPNP catalyzes the transformation of allopurinol (**3**) to its N9 riboside (Allo-Rib)[5] and herewith does not contain L-serine in the catalytic center; indeed, the corresponding β5-sheets of the hPNP TLVVT^{114}N^{115}AAGG and *E. coli* PNP KIIRVGS^{9}CGA[9] allow suggesting the threonine T^{114} or asparagine N^{115} residues of hPNP as key amino acid residues in the synthesis of Allo-Rib; 3) formycin B (Figure 2) was shown to be a good inhibitor of the WT *E. coli* PNP[7a,b] owing likely to the strong hydrogen bonding of Asp204/N1H and C7=O as well as Ser90/N2H,[2,10] but formycin B is inert against hPNP[7a,c,d] implying an inability of the T^{114} or N^{115} residues of the catalytic site of hPNP to assume the Ser90 function of *E. coli* PNP and a low binding efficiency between Asn243/N1H and C7=O as well.

The kinetic parameters obtained and the aforementioned discussion led us to suggest an additional role of the Ser90 residue of the catalytic site of the WT *E. coli* PNP in the binding and/or activation of hypoxanthine. To shed light on the strong influence of the Ser90 on the affinity of hypoxanthine for the WT *E. coli* PNP, we studied the kinetics of the reverse reaction of phosphorolysis of inosine (Table 2). Similar to the synthesis reaction, the inosine affinity (K_m), as well as the maximum initial velocity (V_{max}) and the turnover number (k_{cat}) decreased by 177, 5.4, and 5.5 times, respectively, at transition from the wild-type PNP to the mutant enzyme. One can hypothesize that in the case of natural substrates the Ser90 residue participates in the substrate binding at the catalytic site of the WT *E. coli* PNP, whereas this function is reduces or is

not operative upon interaction with some analogues (see below).

As distinct from 5-aza-7-deazaguanine (**8**), its structural isomer 5-aza-7-deazaisoguanine (**22**) displayed very low substrate activity as it was observed by Voegel et al. in the study on the enzymatic synthesis of its β-D-ribo- and 2′-deoxy-β-D-ribo-nucleosides.[15] A bacterial PNP of unknown origin (Sigma) was used as biocatalyst and the relevant N7-methyl nucleosides **23** as the pentofuranose donors. It was found that the reactions proceed very slowly and 5-aza-7-deazaisoguanosine (**24a**) and its 2′-deoxy counterpart **24b** were obtained in 22 (10 d incubation!) and 54% (in five consecutive reaction cycles!) yield, respectively (Figure 5).

The reason for such a low substrate activity of 5-aza-7-deazaisoguanine (**22**, $^{5A:7DA}$*i*Gua) is difficult to understand. Indeed, an equilibrium of the tautomers **22a** and **22b** is biased towards the sp^2-hybridized N9 tautomer **22b** and its quantum

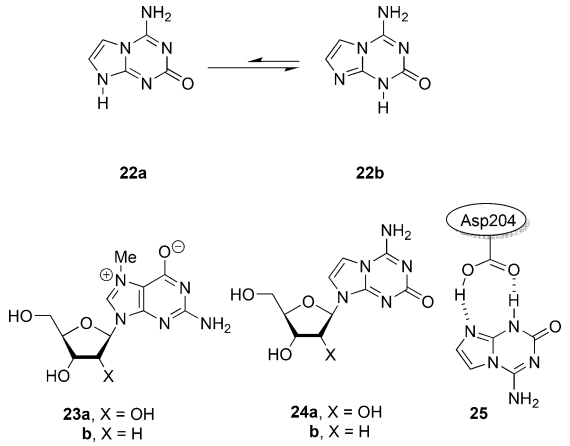

Figure 5. Structures of the tautomers **22a** and **22b** of 5-aza-7-deazaisoguanine (**22**, $^{5A:7DA}$*i*Gua) and its nucleosides **24**. Hypothetical structure of the heterocyclic base binding with Asp204 (**25**, N9 sp^2 character) inhibiting the enzymatic glycosylation.

chemical parameters (e.g., the partial charge of −0.636 e) (Table S1 in the Supporting Information) are in favor of its higher substrate activity versus that of 5-aza-7-deazaguanine (**8**) (see, Table S2 in the Supporting Information). These contradictory data allow us to suggest the formation of the wrong binding complex **25** between the base and the Asp204 side chain of the bacterial PNP catalytic site (see reference [11]), which consists of two strong hydrogen bonds dominating over one correct C6–N(H$_2$)···HO–Cβ(=O)–Asp204 hydrogen bond. However, similar structures with wrong hydrogen binding can apparently exist in the case of 5-aza-7-deazaguanine (**8**) and the natural purine bases with the most populated tautomers characterized by the sp^3-hybridized N9 and sp^2 hybridized N3 atoms, respectively. To assess such a probability of the existence of such erroneous complexes, the structures of 5-aza-7-deazaguanine (**8a**, $^{5A:7DA}$Gua) and its isomer **22b** ($^{5A:7DA}$*i*Gua) with acetic acid as a mimic of the wrong Asp204/base interaction, as well as guanine (Gua) and 8-aza-7-deazaguanine ($^{8A:7DA}$Gua) (both bases populated predominantly in the sp^3-hybridized N9 tautomers) were analyzed by the restricted Hartree–Fock (RHF) ab initio method by using the basis set of the 6-31** FIREFLY QC package,[22] which is partially based on the GAMESS (US)[23] source code (see, also reference [1]) and the selected data are presented in Table 3. Note that all the four analyzed bases have analogous empirical formula.

The hydrogen-bonded structure $^{5A:7DA}$Gua-N9H/AcOH was found to be thermodynamically most stable among the complexes analyzed taking into account the total energy values. This result contrasts with a unique substrate activity of 5-aza-7-deazaguanine, which surpasses all the studied compounds, including guanine. Notably, the probability of substrate binding in the active site of the enzyme as shown for guanine was previously proven by us on an example of 2′-deoxyglycosylation of N^2-acetylguanine, wherein initially the N7 glycoside was formed, which rearranges into the thermodynamically more stable N9 glycoside.[20] Such a course of the enzymatic glycosy-

Table 3. Geometry-optimized structures of the most populated tautomers of 5-aza-7-deazaguanine (**8**, $^{5A:7DA}$Gua, sp^3-hybridized N9 atom) and 5-aza-7-deazaisoguanine (**22**, $^{5A:7DA}$*i*Gua, sp^2-hybridized N9 atom) in double wrong hydrogen bonding with acetic acid as a mimic of the Asp204 binding at the catalytic site of the *E coli* PNP; similar hypothetic structures of guanine and 8-aza-7-deazaguanine ($^{8A:7DA}$Gua) (both in the most populated sp^3-hybridized N9 form) are calculated for comparison reason.

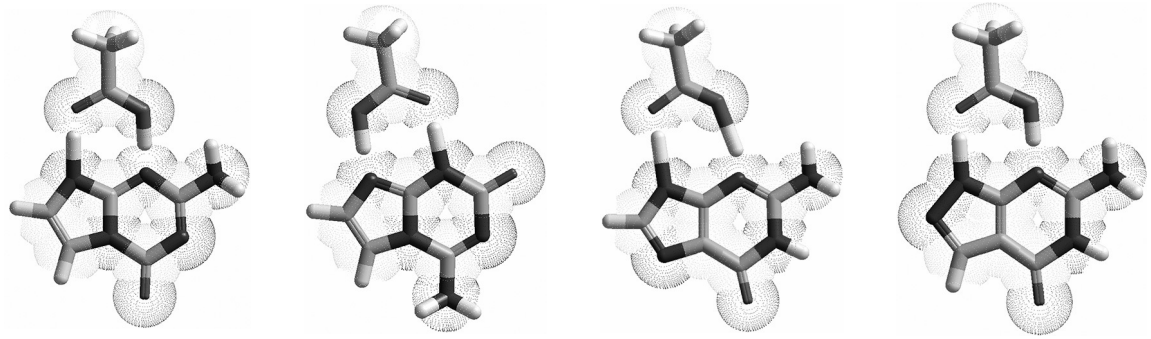

	$^{5A:7DA}$Gua-N^9H(sp^3)/AcOH	$^{5A:7DA}$*i*Gua-N^9(sp^2)/AcOH	Gua-N^9H(sp^3)/AcOH	$^{8A:7DA}$Gua-N^9H(sp^3)/AcOH
E_T [kcal mol^{-1}]	−48 1585.3	−48 1570.1	−48 1579.3	−48 1570.3
E_{HOMO} [eV]	−8.8846	−8.9825	−8.0383	−8.5091
E_{LUMO} [eV]	3.5674	2.5824	3.3851	3.2572

lation is excluded in the case of the other three bases, and their glycosylation depends on several factors, particularly the ability of the Asp204 side chain to bind the C6 carbonyl group of the substrate. Surprisingly, the values of E_{LUMO} satisfactorily correlate with the substrate properties of the analyzed set of bases, wherein $^{5A:7DA}$*i*Gua-N9/AcOH with the lowest substrate activity is characterized by the lowest value of E_{LUMO} (see below).

Substrate activities of the new 8-aza-7-deazapurines towards the WT *E. coli* PNP

To validate the area of the enzymatic synthesis of 8-aza-7-deazapurine nucleosides, the substrate activity of 8-aza-7-deaza-2-fluoro-6-methylthiopurine (**5**), 8-aza-7-deaza-2,6-diaminopurine (**6**),[24a] and 6-amino-8-aza-7-deaza-2-fluoropurine (**7**) towards the WT *E. coli* PNP was tested and the data for the complete set of the analogues were analyzed from viewpoint of their electronic structure (Tables S1 and S2 in the Supporting Information). The fluoride **7** was synthesized from the diamino heterobase **6** by the Schiemann reaction in 21% yield (Scheme 1).

Unexpectedly, the base **5** showed no substrate activity for the WT *E. coli* PNP. On the contrary, the enzymatic 2-deoxyribosylation of the bases **6** and **7** proceeds with high efficiency

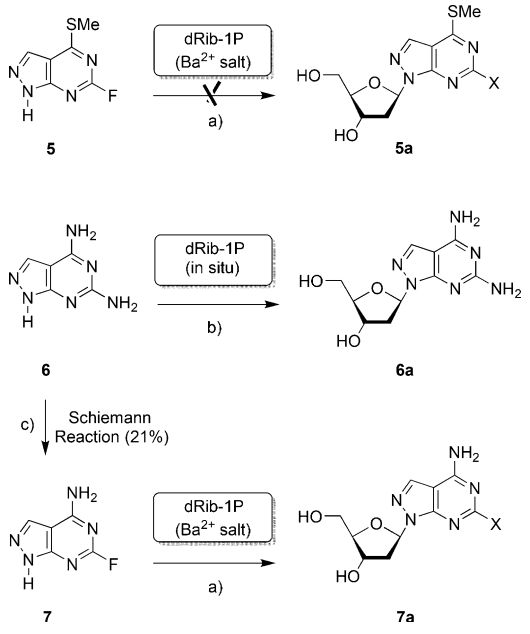

Scheme 1. Reaction conditions: a) Synthesis of dRib-1P: incubation of thymidine in K/phosphate buffer (0.5 M) at 50 °C for 12 h in the presence of *E. coli* TP gave rise to the phosphorolysis of the starting nucleoside in approximately 80% yield (HPLC). Workup followed by the final treatment with $Ba(OAc)_2$ afforded the desired phosphate in 37% yield; the latter was used in the synthesis of compound **7a** (2 mM Tris·HCl (pH 7.2) 23 °C, 2 h) (95%). b) In situ dRib-1P was obtained from thymidine (0.2 M K/phosphate buffer (pH 7.4) at 40 °C for 1 h) in the presence of *E. coli* TP to give approximately 95% conversion of thymidine to thymine and dRib-1P; the base **6** and *E. coli* PNP were added to this reaction mixture; 40 °C, 18 h (71%); c) 70% HF/pyridine, −11 °C and an aqueous solution of KNO_2 for 1 h; −11 °C→6 °C for 2 h (21%).

and the corresponding nucleosides **6a** and **7a** were detected by HPLC/mass spectrometry analysis in the reaction mixtures in 95–98 yields. The synthesis of the nucleoside of 8-aza-7-deaza-2,6-diaminopurine (**6**) that is an analogue of 2,6-diaminopurine (DAP) is of interest for further study of its chemistry and enzymatic transformations, which are developed for DAP and its nucleosides, to obtain potentially biologically important nucleosides, for example, nucleosides of 6-amino-8-aza-7-deaza-2-fluoropurine (**7**), and oligonucleotides. It is noteworthy that the chemical glycosylation of 8-aza-7-deazapurines resulted in the formation of the N9 and N8 regioisomeric nucleosides, which is a significant drawback of chemical protocols (see e.g., reference [24]).

The transglycosylation of the base **6** by using a combination of thymidine/thymidine phosphorylase (TP)[16] for an in situ generation of 2-deoxy-α-D-ribofuranose-1-phosphate (dRib-1P) as well as *E. coli* PNP[16] gave, after workup and silica gel column chromatography, the desired nucleoside **6a** in 71% yield. The formed thymine formed and nucleoside **6a** were coprecipitated from the reaction mixture and isolation of the pure nucleoside **6a** from this mixture needed careful and laborious chromatography. Keeping this in mind, the synthesis of nucleoside **7a** was realized in two steps: the preparation of dRib-1P from thymidine in the presence of *E. coli* TP that was isolated as stable barium salt in 37% yield (see reference [25]) and then condensation with the base **7** affording nucleoside **7a** in 95% yield after conventional silica gel column chromatography.

The pure individual α anomer of dRib-1P (Ba^{2+}, purity > 97%) was found to be stable at room temperature and its ^{1}H, ^{13}C, and ^{31}P NMR spectra are in fair agreement with the expected structure, albeit some coupling constants differ from the corresponding constants obtained for the cyclohexylammonium salt.[26] The structure of the synthesized nucleosides **6a** and **7a** were proven by the integrity of spectral methods (UV, ^{1}H, and ^{13}C NMR spectroscopy as well as mass spectrometry). Treatment of the 2,6-diamino nucleoside **6a** with adenosine deaminase (ADA from calf intestine, Sigma) resulted in a gradual transformation into 8-aza-7-deaza-2′-deoxyguanosine as it was monitored by the changes of the UV spectra characterized by two isobestic points at $\lambda = 235$ and 267 nm (see reference [24] as well as Figure S1 in the Supporting Information).

It is obvious that the trans-2-deoxyribosylation studied depends on the electronic structure of the heterocyclic bases that was analyzed for the complete set of 8-aza-7-deazapurines studied as described above in comparison with the corresponding purine bases (Table S1 in the Supporting Information). Noteworthy that the sp^3-hybridized N9 tautomers prevail over the sp^2-hybridized N9 tautomers in the case of 8-aza-7-deazapurines (except allopurinol) and the partial negative charges of the sp^2-hybridized N9 tautomers of the purines are significantly higher (absolute values!) than the one of the corresponding nitrogen atoms of 8-aza-7-deazapurines, which is generally consistent with a higher substrate activity towards the WT *E. coli* PNP.

Electronic structure of the 8-aza-7-deazapurines and their complexes with the Ser90 side chain of *E. coli* PNP

An ab initio analysis of the electronic structure of the bases **2**, **4**, and **5** showed that the C6 oxygen atom of the former is negatively charged, whereas the corresponding chlorine and sulfur atoms of the latter ones are positively charged, precluding the hydrogen bonding with Asp204. Previously, it has been shown that purine heterocycles having thioalkyl or mercapto substituents at the C6 atom are substrates similar to the corresponding oxygen-containing purines[17,27,28] apparently due to the Asp204/N7 hydrogen bonding at the catalytic site of the PNP. Moreover, we have recently shown that the WT *E. coli* PNP accepts a number of purine bases with bulky C6 substituents (e.g., kinetin, N^6-benzoyl- and N^6-benzyladenines, N^2-acetyl-O^6-methyl- and N^2-acetyl-O^6-benzylguanines, or N^2-acetyl-O^6-[2-(4-nitrophenyl)ethyl]guanine) as substrates in the transglycosylation reactions pointing to a large hydrophobic space close to the C6-N1-C2 segment of the pyrimidine ring of the purine derivatives in the active site that can accommodate these groups.[28–30] In addition, we have shown that 1-deazapurines, 3-deazapurines, and 1,3-dideazapurines (benzimidazole) are good substrates of the WT *E. coli* PNP.[31–35] These data point to a modest contribution of the C6 amino- or oxygen-containing functions of the purines in the substrate binding and presumably its activation.[32,33] However, in the case of 8-aza-7-deazapurines the Asp204···O(N)–C6 interactions were assumed to become operational for the binding of the substrate in the catalytic site of *E. coli* PNP,[1] the value of which can be assessed indirectly by testing such compounds as the C6–Cl and –SMe derivatives **4** and **5**.

Comparison of the tautomeric structure of the bases **4** and **5** resulting from the geometry optimization (Table S1 in the Supporting Information) shows a close similarity as for the prevailing population of the sp^3-hybridized =N8–N9H–C4 tautomer ($\Delta E_T = -11.5$ and 10.3 kcal mol^{-1}, respectively) as well as the partial charges of the sp^2-hybridized N9 (–N8(H)–N9=C4, −0.422 and −0.398 e, respectively) and the N8 (=N8–N9(H)–C4, −0.279 and −0.273 e, respectively) nitrogen atoms. Taking into account that 1) neither the chlorine nor the sulfur atom of the respective bases **4** and **5** is able to interact with the β-carboxyl group of Asp204, and 2) the steric hindrances created by the SMe group for the substrate binding at the catalytic site appear to be minimal (see above), these data do not allow to make reasonable conclusion regarding the absence of substrate activity of the base **5** as compared with the satisfactory substrate activity of the chloride-containing base **4**.

Analysis of the quantum chemical parameters of the studied bases in a complex with the Ser90 side chain (Figure 6, binding vs. productive complex) by the restricted Hartree–Fock ab initio method[22,23] (see, also reference [1]) led to interesting observations (Table S2 in the Supporting Information). Among the energy values of the highest occupied molecular orbital (HOMO), the lowest unoccupied molecular orbital (LUMO), and the HOMO–LUMO gap describing the electronic structures of the 8-aza-7-deaza-purines **1**–**7**, only the E_{LUMO} parameters manifest a qualitative correlation with the substrate properties of the bases, that is, the base **5** with the lowest E_{LUMO} value of 2.119 eV (the binding) and 1.640 eV (the productive complex) showed no substrate activity for the WT *E. coli* PNP (see, e.g., with the HOMO and the LUMO analysis by Pearson[36]). Noteworthy, 1) that the hydrogen-bonded complex of $^{5A:7DA}$*i*Gua-N9/AcOH showed the lowest E_{LUMO} value (see above), which is in harmony with the lowest substrate activity of $^{5A:7DA}$*i*Gua versus the related bases (Table 3), and 2) that the LUMO energy level was shown to be one of the most informative quantum chemical parameters in the correlation of biochemical properties (see, e.g., references [37–39]). A similar dependence of the substrate activity of 8-aza-7-deazapurines on the ΔE value of the hardness of binding ($2\eta B$) and productive complex ($2\eta PC$)[40] was observed, that is, the calculated ΔE value of 0.320 eV for compound **5** is the lowest value among the analogues studied.

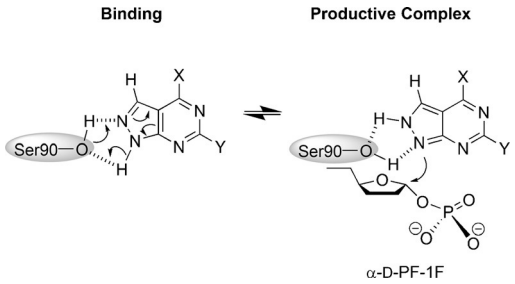

Figure 6. Structures of the heterocyclic base binding with Ser90 (N9 has sp^3 character) and transformation to the productive complex (N9 has sp^2 character).

The value of $\Delta E = 2\eta B - 2\eta PC$ of −0.238 eV for the prevailing C6=O keto tautomer of allopurinol (Table S2 in the Supporting Information) is entirely different from a number of the corresponding values calculated for all other heterocycles studied. Unexpectedly, the ΔE value of 0.452 eV for the less populated C6–OH tautomer is in agreement with similar data for other bases. Presently, we have no arguments in favor of this structure as the real hypoxanthine tautomer at the catalytic site of *E. coli* PNP.

Recognition of the challenging heterocyclic bases by the wild-type *E. coli* PNP versus its Ser90Ala mutant—7-thia motif and 7-thia/α-amino group combination

Among the unnatural heterocyclic compounds showing substrate activity for *E. coli* PNP, *N*-(1,3,4-thiadiazol-2-yl)-cyanamide (LY217896, **26**) (Figure 7) occupies an exclusive position because it has no structural elements reminiscent of any natural heterocyclic bases, and nevertheless, is an excellent substrate for both the mammalian and the bacterial (Sigma) PNP, and moreover, the formation of two regioisomeric ribosides, that is, the N4- and N3-β-D-ribofuranosides **26a** (reversible synthesis!) and **26b** (irreversible ribosylation) was observed in the presence of α-D-ribofuranose-1-phosphate (Rib-1P)[41,42] (reviewed in [4a]).

The quite puzzling substrate activity of the thiadiazole **26** for the PNPs of diverse origin prompted us to test the sub-

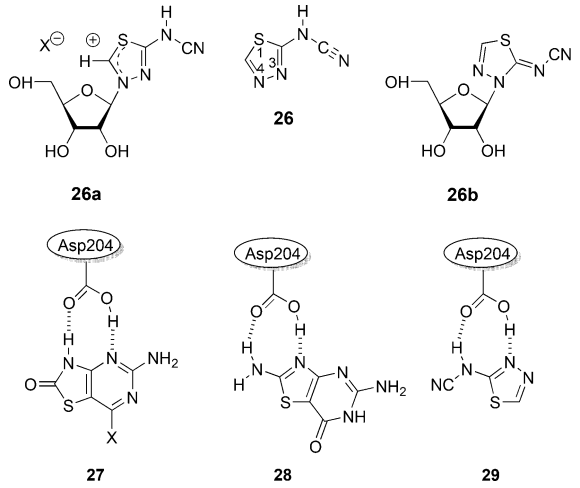

Figure 7. Structures of *N*-(1,3,4-thiadiazol-2-yl)-cyanamide (LY217896, **26**) and its regioisomeric ribosides **26a** and **26b**, as well as the supposed hydrogen bonding of the purine analogues with the Asp204 residue in the catalytic site of the *E. coli* PNP.

strate properties of 8-oxo-7-thiaguanine (**10**), 8-amino-7-thiaguanine (**11**), and 8-chloro-7-thiaguanine (**12**) as well as 7-thiaxanthine (**13**), 9-deaza-7-thiaxanthine (**14**), and its 2′-deoxyriboside **14a** (Figure 1), keeping in mind that these structures vaguely resemble the five-membered ring of the thiadiazole **26**. Unfortunately, all the 7-thiaguanine derivatives **10**–**12** showed extremely low substrate activity in the transribosylation and trans-2-deoxyribosylation reactions catalyzed by the wild-type and Ser90Ala mutant *E. coli* PNPs. In experiments with the 8-oxo derivative **10**, careful HPLC analysis by using chemically synthesized nucleosides as standards, allowed us to identify the nucleoside peaks; however, the yield of the nucleosides was on the level of 1–2%. By analogy with 5-aza-7-deaza-iso-guanine (**22**) (Figure 5), miserable substrate activity of the 7-thiaguanine derivatives **10** and **11** along with modest inhibition of the PNP-catalyzed inosine synthesis (see below) are presumably due to the formation of wrong complexes of the bases with the Asp204 residue (see structures **27** and **28** in Figure 7).

The lack of substrate activity of 8-amino-7-thiaguanine (**11**) for the *E. coli* PNP was the most unexpected finding, because according to the ab initio analysis (6-31G**, the basis set of parameters) its most populated tautomer is characterized by the sp^2-hybridized structure of the N9 atom (two thermodynamically equivalent C6 oxo/hydroxy forms) with a partial charge of −0.612 e as distinct from 8-oxo-7-thiaguanine (**10**) that preferably populates in the C8=O oxo form, thereby precluding the nucleophilic attack on the C1 atom of an α-D-pentofuranose-1-phosphate (Table 4) (Table S3 in the Supporting Information).

Doskocil and Holy found that 8-aminoguanosine is a good substrate towards the *E. coli* PNP, comparable to the corresponding natural substrate guanosine,[17] and a poor inhibitor of guanosine phosphorolysis by the same enzyme. It was reasonably to expect the similar situation in the case of an enzymatic glycosylation of 8-amino-7-thiaguanine (**11**), that is, the C8 amino function will not create any additional hindrances to the formation of the productive substrate–enzyme complex. On the other hand, the formation of a Ser90/C8–NH_2 hydrogen bond is a highly probable event, however, the impact of this event on the formation of glycosyl linkages is difficult to predict (see below).

The chloride **12** and 7-thiaxanthine (**13**) (see reference [43]) showed no substrate and inhibitory properties for the *E. coli* PNP despite the fact that they exist in the N9 imino tautomers (partial charges of −0.470 and 0.512 e, respectively) (Table S3 in the Supporting Information) demonstrating thereby a very low affinity to the catalytic site of the *E. coli* PNP. 8-Oxo-7-thiaguanine (**10**) and 8-amino-7-thiaguanine (**11**) showed a moderate affinity to the catalytic site of the WT *E. coli* PNP in experiments on the synthesis of inosine from Rib-1P (barium salt) and hypoxanthine in the presence of equimolar concentrations of both bases. The velocity of the inosine formation was reduced by 7 and 16%, respectively, pointing to the modest competition of the 7-thiaguanines **10** and **11** for the catalytic site of the enzyme (data not shown). Moreover, we found that uric acid, existing in multiple hydroxy/oxo tautomeric forms,[44] is the modest substrate for the *E. coli* PNP, which catalyzes the synthesis of N9 riboside[45] in the reaction with Rib-1P in 12% yield; it is likely that one of tautomeric forms with a sp^2-hybridized N9 atom is populated in the aqueous reaction buffer enabling the formation of a glycosyl bond (this work is in progress).

Table 4. Geometry-optimized (ab initio method, 6-31G**, basis set of parameters, HyperChem 8.1) structures of the two tautomers of 8-oxo-7-thiaguanine (**10**) and 8-amino-7-thiaguanine (**11**).

	Most stable tautomer		Less stable tautomer	
	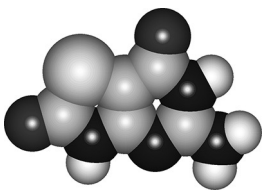	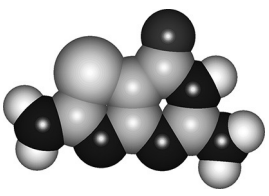	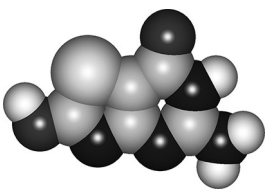	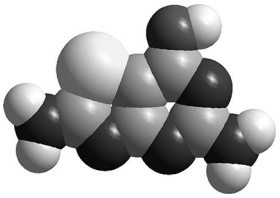
E_T [kcal mol^{-1}]	−600 386.3[a]	−587 933.5	−600 368.1	−587 933.4

[a] $\Delta E = -18.5$ kcal mol^{-1}.

The differences in the substrate properties of uric acid versus the 7-thiaguanines **10** and **11** can be attributed to 1) a more efficient binding and correct docking at the catalytic center of the PNP of the former through two Asp204/base hydrogen bonds, and/or 2) a stringent control of the space dimensions of the substrate molecule. Regarding the latter, the discussed differences of the substrate properties can be attributed to the known differences in the van der Waals radii of the N7 nitrogen atom of uric acid versus a sulfur atom of compounds **10** and **11**.

Comparative ab initio analysis of the electronic structures of 8-amino-7-thiaguanine (**11**) and *N*-(1,3,4-thiadiazol-2-yl)-cyanamide (**26**) and two modes of an overlay of the geometry-optimized structures show a close similarity of both five-membered rings. The lack of substrate activity of the former remains obscure. Indeed, by assuming for the nucleoside **26** similar hydrogen bonding as proposed for the base **11** (Figure 7, structure **29**), one would expect a similar inhibitory activity (Table 5, right overlay), but this is contrary to the known substrate properties of the thiadiazole **26**. Apparently, the correct positioning of the thiadiazole **26** in the catalytic center of the PNP, which enables the attack of both nitrogen atoms at the C1 atom of the Rib-1P, is implemented through an interaction of the exocyclic –N(H)–C≡N group with the Asp204 residue (Table 5, left overlay). It is logical to suggest that the binding of the base **11** through the C6 carbonyl group/Asp204 hydrogen bond, if it is realized at all, leads to a spatial arrangement of the substrate at the catalytic center that is not compatible with the PNP requirements, whereas the unique binding through the cyanamide group in the catalytic site of the PNP enables a nucleophilic attack of both sp^2-hybridized nitrogen atoms, that is, N3 and N4, on the anomeric C1 atom. Anyway, testing of the substrate properties of heterocyclic compounds having cyano or acetylene group for *E. coli* PNP is of obvious interest.

Table 5. Geometry optimization by the ab initio method (6-31G**) of 8-amino-7-thiaguanine (**11**) and *N*-(1,3,4-thiadiazol-2-yl)cyanamide (**26**) and overlay of the five-membered rings of both structures.

8-Amino-7-thiaguanine	*N*-(1,3,4-Thiadiazol-2-yl)cyanamide
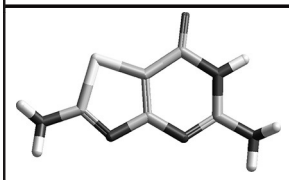	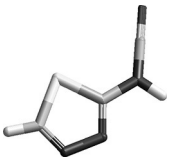
partial charges of selected atoms [e]	
N9 = −0.612	N3 = −0.351
S7 = +0.303	N4 = −0.226
O6 = −0.625	S1 = +0.311
two kinds of overlay of both structures	
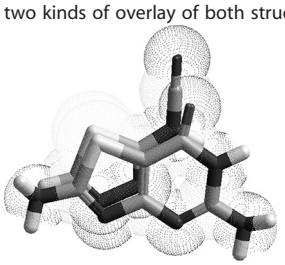	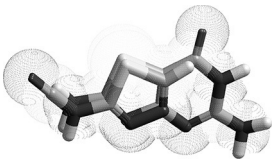

9-Deaza-7-thiaxanthine (**14**) and its 2′-deoxyriboside **14a** did not inhibit the phosphorolysis of inosine (1:1 (mol) inosine/inhibitor ratio, 0.1 M phosphate buffer (pH 7.3), 20 °C, time of reaction 10 min). The lack of activity of the heterocyclic base **14** is consistent with data obtained for the related 7-thiapurines **10**–**13** and its glycosylation does not result in an increased affinity for the enzyme.

9-Deazapurines and their nucleosides as valuable probes of the Ser90/N9 inosine co-operation

To evaluate the efficiency of the Asp204 and N7H/C6=O double hydrogen binding, we studied the phosphorolysis of inosine (see references [46,47]) under standard reactions conditions in the presence of 9-deazaxanthine (**15**) and 9-deaza-9-iodoxanthine (**16**) as well as the 2′-deoxy-β-D-ribonucleosides of 9-deazaxanthine (**17**) and 9-deazaguanine (**18**), the syntheses of which were published recently.[48,49] Compounds of this group do not contain a substituent at the C8 atom and this allows eliminating of the consideration of interactions with the Ser90 side chain. It was found that 9-deazaxanthine (**15**) and its 2′-deoxy-β-D-riboside **17** exhibited weak inhibitory activity (13–15% inhibition) and 9-deaza-9-iodoxanthine (**16**) remarkable activity (77% inhibition) in the phosphorolysis of inosine; 9-deaza-2′-deoxyguanosine (**18**) as opposed to 9-deaza-2′-deoxyxanthosine (**17**) did not inhibit the inosine phosphorolysis under standard reaction conditions. Differences in the inhibitory properties of the nucleosides **17** and **18** reflect apparently different electronic properties of the H7N–C5–C6=O fragments of the corresponding aglycones, which determine the efficiency of their interaction with Asp204 by the formation of two hydrogen bonds and the ability to compete with similar inosine hydrogen bonds.

At first glance, a significantly higher inhibitory activity of the iodide **16** in comparison with the parent base **15** is unexpected. However, it was previously shown that 5′-deoxy-5′-iodo-9-deazainosine is a significantly more effective competitive inhibitor of hPNP from human erythrocytes than the parent compound 9-deazainosine,[46] which corresponds to the behavior of the bases **15** and **16**, and reveals a certain similarity of the two PNPs. Kinetics of the inosine phosphorolysis by the *E. coli* PNP was studied by the conventional initial velocity method as well as with the use of three concentrations of the iodide **16** and the data are displayed by Lineweaver–Burk plots (Figure 8).

The Michaelis–Menten constant, $K_M = 23.3$ μM, the maximal velocity $V_{max} = 0.70$ μM min^{-1} mg^{-1}, and $k_{cat} = 67$ sec^{-1} were calculated for the inosine phosphorolysis. Unlike 5′-deoxy-5′-iodo-9-deazainosine,[46] a non-competitive or rather a mixed type of inhibition of the inosine phosphorolysis was established in the case of iodide **16** with respect to the nucleoside substrate. It was found that the phosphorolysis in the presence of the inhibitor is accompanied by a decrease in the V_{max}/K_M ratio and therefore the inhibition constant ($K_i = (10 \pm 1)$ μM) was calculat-

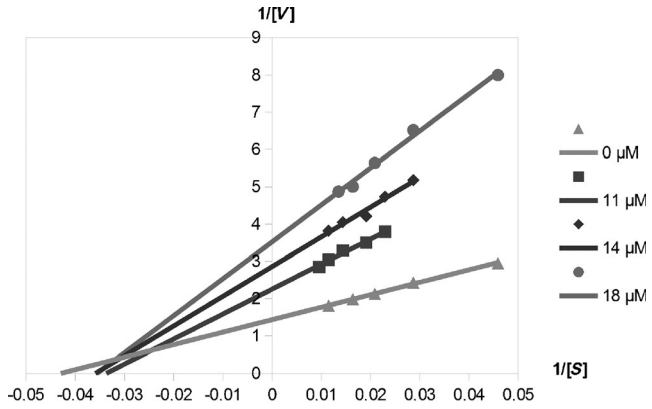

Figure 8. Double reciprocal plot (1/[*V*] vs. 1/[*S*]) for the inosine phosphorolysis in the presence of 0, 11, 14, and 18 μM of 9-deaza-9-iodoxanthine (**16**). All the reactions were run in 0.1 M K/phosphate buffer (pH 7.3) at 20 °C for 10 min, 93 $\mu g L^{-1}$ of the PNP with an activity of 27 $U mg^{-1}$, 35–105 μM of inosine. The progress of the phosphorolysis was monitored at $\lambda = 248$ nm ($\Delta\varepsilon = 3160\ M^{-1} cm^{-1}$).

ed as it was suggested by Shugar et al.[47] One can hypothesize that a non-specific binding of the 5′-iodo substituent within the amino acid residue(s) of the exocyclic 5′-OH binding site of the hPNP contributes to the strong anchoring of the rest of the molecule at the catalytic site. On the contrary, a similar non-specific binding of the base **16** prevails over the specific double hydrogen bonding of the *E. coli* Asp204 side chain with the HN–C–C=O fragment of the base.

The most surprising finding was the weak inhibitory activity of 9-deaza-2′-deoxyxanthosine (**17**) and furthermore, the lack of such activity of the 9-deazaguanine analogue **18**. Indeed, the nucleosides **17** and **18** have all the functional groups necessary for an efficient binding in the active site of the *E. coli* PNP. One can assume that the *E. coli* PNP requirements to the spatial arrangement of the substrate at the catalytic center are significantly different from those of the human enzyme, and, apparently, the nucleosides **17** and **18** are unable to adopt the necessary stereochemistry for the docking in the active center (for a detailed discussion of peculiar stereochemistry of the *N*- vs. *C*-nucleosides, see Chattopadhyaya et al.[50]). An alternative explanation is that the Ser90 residue of the *E. coli* PNP plays an essential role in linking the nucleoside substrate by a hydrogen bond between the Ser90–OγH hydroxyl group and the N9 atom of natural purine nucleosides. The latter assumption is consistent with the data presented above (Table 2) for the phosphorolysis of inosine by the wild-type *E. coli* PNP and a mutant enzyme, wherein a significant decrease of the PNP affinity was found by replacing the Ser90 residue by L-alanine. These suggestions are of undoubted interest and deserve more detailed study.

Benzimidazole and its 2-amino derivative as well as their 3-thia- and 3-oxa derivatives as probes of the role of the PNP Ser90 residue in the enzymatic glycosylation

To minimize the contribution of the pyrimidine ring of the purines in the reactions catalyzed by the *E. coli* PNP and its mutant, the substrate properties of benzimidazole (**19**), 1,3-benzothiazole (**20**), and 1,3-benzoxazole (**21**), as well as their respective 2-amino derivatives **19a** (^{NH_2}BI), **20a** (^{NH_2}BS), and **21a** (^{NH_2}BO) (Figure 1) towards the wild-type and mutant *E. coli* PNPs were studied. Selection of these bases was made to obtain complementary data with regard to the exocyclic amino motif in a combination with the endocyclic amino, sulfur, and oxygen substitution in the five-membered ring in the recognition of the bases by the *E. coli* PNP. The substrate properties of these compounds (except BI) towards the *E. coli* PNP have not, to our knowledge, been studied before and are of interest for the reason that they differ only by one substituent in the five-membered ring and enable to eliminate the contribution of the pyrimidine ring substituents in the enzymatic reactions under consideration.

Benzimidazole was studied for comparison reason and taken as a substrate, the high activity of which for *E. coli* PNP was shown previously.[31–33] The standard reaction conditions for the transglycosylation of the complete set of bases were employed based on the BI transribosylation data. A combination of the *E. coli* uridine phosphorylase (UP)[16] and uridine or 2′-deoxyuridine was used for an intermediary generation of α-D-ribo-furanose-1-phosphate (Rib-1P) or α-D-2-deoxyribo-furanose-1-phosphate (dRib-1P) in the synthesis of the respective ribo- and 2′-deoxyribonucleosides.

The formation of the ribonucleosides (**31a**, Figure 9, A) and the 2′-deoxyribonucleosides (**31b**,Figure 9, C) of BI catalyzed by the WT *E. coli* PNP proceeded very quickly and the main difference between both reactions consisted in the changes of the base/nucleoside ratio that occurred during long-term storage of the reaction mixtures. Thus, the quantitative transformation of BI into 1-(2-deoxy-β-D-ribofuranosyl)benzimidazole (dRib-BI) (Figure 9, C) occurred in a few minutes and then the concentration of dRib-BI in the reaction mixture decreases gradually until approximately 15% after 140 h. On the contrary,

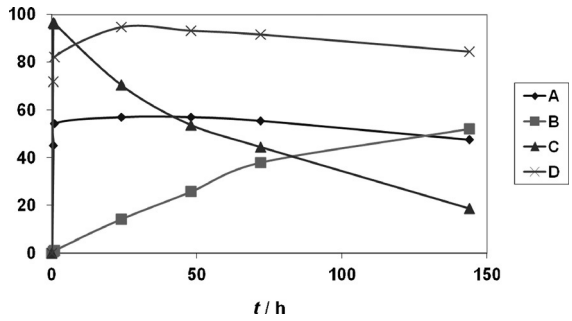

Figure 9. Progress of the synthesis of benzimidazole nucleosides PNP Rib-BI and dRib-BI (in [%], ordinate) by using the WT *E. coli* PNP (A = Rib-BI, C = dRib-BI) versus the mutant PNP (B = Rib-BI, D = dRib-BI) (HPLC analysis). Reaction conditions: a) Synthesis of the ribosides: reaction mixture (1 mL) contained the base (2 mM) and uridine (2 mM) in K/phosphate buffer (2 mM, pH 7.0). b) Synthesis of the 2-deoxyribosides: reaction mixture (1 mL) contained the base (2 mM) and 2′-deoxyuridine (4 mM) in K/phosphate buffer (4 mM, pH 7.0). The reactions were initiated by addition of the recombinant *E. coli* enzymes: UP (0.036 $mg mL^{-1}$, 3.6 units) and the *E. coli* PNP (0.06 $mg mL^{-1}$, 3.24 units) or the mutant PNP (0.06 $mg mL^{-1}$, 0.072 units) and the reaction mixtures were incubated at 50 °C.

the formation of Rib-BI (Figure 9, A) quickly attained around 55% and the equilibrium BI+Rib-1P⇄Rib-BI+Pi remained unchanged in the reaction mixture during 144 h (Figure 9).

In reactions catalyzed by the mutant enzyme, the formation of dRib-BI (Figure 9, D) attained approximately 95% yield after 24 h and further maintaining the reaction is accompanied by the very slow decrease of the product concentration to around 83%. Ribosylation of BI (Figure 9, B) was running very slowly and yet reached approximately 50% output after 144 h of incubation.

The high efficiency of the BI deoxyribosylation is fully consistent with the results obtained previously in similar experiments.[31] The enzymatic synthesis has an equilibrium nature and the decline of the dRib-BI concentration obtained by using the *E. coli* PNP (Figure 9, C) versus the use of the mutant PNP (Figure 9, D) indicates complementary WT PNP activity (see references [51, 52]), which catalyze 2-deoxy-α-D-ribofuranse-1-phosphate dephosphorylation. The intermediary α-D-ribofuranse-1-phosphate is more resistant against this side activity of the WT *E. coli* PNP under reaction conditions used. It was supposed that the Ser90 residue of the *E. coli* PNP takes a part in the hydrogen bonding with (d)Rib-1P[8, 10] and the side activity of the wild-type enzyme is likely connected with this interaction.

Comparison of the reactions A and B (Figure 9) unequivocally points to the participation of the Ser90 residue of the catalytic site of the WT *E. coli* PNP in the binding/activation of the substrate, just (the same way) as it was mentioned above for the synthesis of inosine. The nature of this positive impact is difficult to imagine, and the replacement of Ser90 with L-alanine leads to a marked slowdown in the synthesis of the riboside BI-Rib (Figure 9, B) catalyzed by the mutant enzyme (Figure 10).

Characteristic features of the synthesis of the ribosides (Figure 9, A and B) and the 2′-deoxyribosides (Figure 9, C and D) of BI catalyzed by the two enzymes are manifested also in the synthesis of the relevant glycosides of 2-aminobenzimidazole, but the efficiency of the synthesis is much lower (Figure 10). It is obvious that the Ser90 residue has a positive effect on the synthetic reactions catalyzed by the wild-type enzyme (Figure 10, A and C), and, like the glycosylation of benzimidazole, 2′-deoxyribosylation (Figure 10, C and D) occurred with greater efficiency than ribosylation (Figure 10, A and B). Again, the decrease of the product concentration in the reaction mixture after attaining the maximal content (Figure 10, C) was observed only in the synthesis of ^{NH_2}BI-dRib catalyzed by the wild-type enzyme. Participation of the Asp204 residue of the catalytic site of the *E. coli* PNP in the binding and activation of ^{NH_2}BI as well as BI appears to be similar to that in the reactions of natural heterocyclic bases.

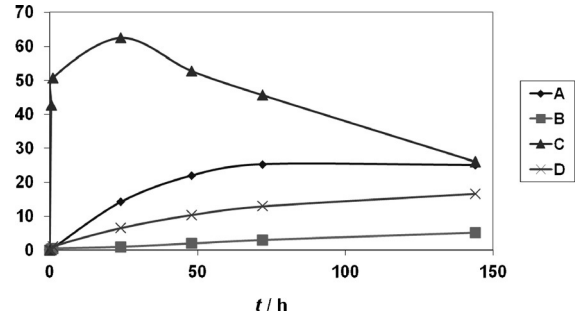

Figure 10. Progress of the synthesis of the ribonucleosides (A and B) versus the 2′-deoxyribonucleosides (C and D) nucleosides (in [%], ordinate) of 2-aminobenz-imidazole by using the WT *E. coli* PNP (A and C) or the mutant PNP (B and D) (HPLC analysis). Reaction conditions: see Figure 9.

To validate the possibility of the practical enzymatic synthesis of ^{NH_2}BI nucleosides, the reaction conditions of the ^{NH_2}BI-dRib (**32b**) synthesis were optimized and the desired compound was obtained in 91% yield (see the Experimental Section).

It is obvious that the binding and activation of BI at the catalytic site of the wild-type and mutant PNPs is realized mainly by the interaction of the Asp204 side chain with one of the endocyclic nitrogen atoms (Scheme 2). It is likely that in the case of the BI glycosylation catalyzed by the *E. coli* PNP a positive contribution of the side chain of Ser90 in the reaction effec-

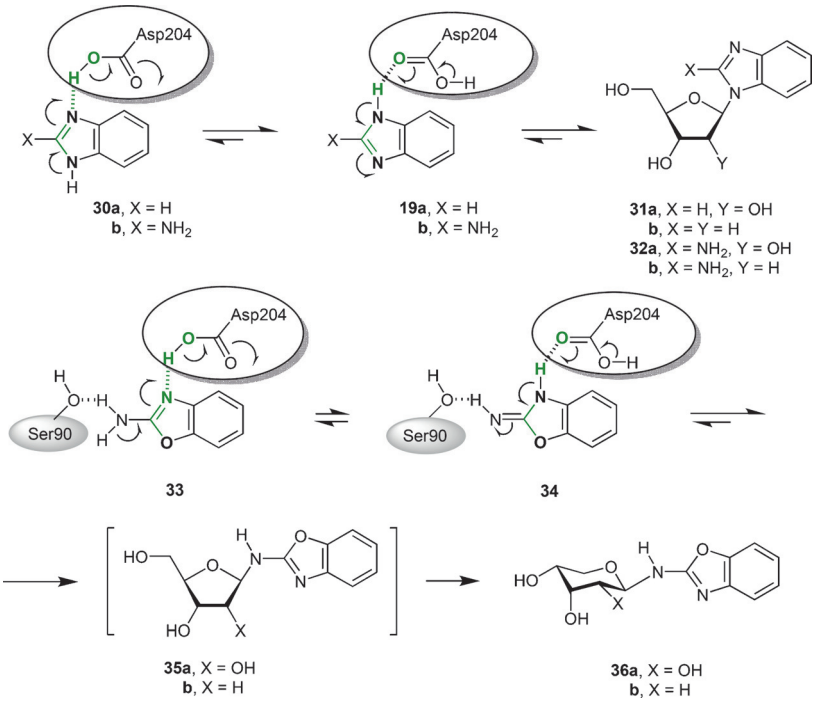

Scheme 2. Suggested structures of hydrogen-bonded heterocyclic bases at the catalytic site of *E. coli* PNP, as well as products of the glycosylation of BI (**31**) and ^{NH_2}BI (**32**), and ^{NH_2}BO **35a** and **35b** and **36a** and **36b**.

tiveness is similar to that of hypoxanthine glycosylation (see above). Lower efficiency of the synthesis of ^{NH_2}BI-dRib (Figure 10, C) versus that of dRib-BI (Figure 9, C) is apparently associated with the cooperation or competition of the two types of substrate binding in the catalytic center of the enzyme, that is, 1) the main binding through protonation of an endocyclic nitrogen atom by the Asp204 side chain (e.g., structures **30** and **19**, Scheme 2) and 2) additional hydrogen-binding C2–NH_2 function with the Ser90 side chain (see structures **33** and **34**, Scheme 2). The latter mode of interaction can also takes place in the case of 2-aminoadenine and thereby increases the affinity to the enzyme as it was stated by Doskocil and Holy:[17] the K_i constants of the phosphorolysis of guanosine in the presence of adenosine and 8-aminoadenosine were found to be 350 and 5.5 μM, respectively. This type of hydrogen bond may also be present in the binding of the 7-thiapurines **10** and **11** at the catalytic site of the *E. coli* PNP, however, if in the case of good substrates such as BI it reduces the reaction rate, in the case of poor substrates the formation of such hydrogen bonding further reduces the probability of the formation of the glycosyl linkage.

Unlike benzimidazole, 1,3-benzthiazole (**20**) and 1,3-benzoxazole (**21**) revealed no substrate activity towards the wild-type enzyme and its mutant as well. In contrast to 2-aminobenzimidazole (**19a**), 2-amino-1,3-benzothiazole (**20a**) showed neither substrate nor inhibitory activities; the latter was tested in the synthesis of inosine pointing to inefficient hydrogen binding at the catalytic site of the wild-type PNP.

The base **21a** showed modest substrate activity in the trans-ribosylation and trans-2′-deoxyribosylation catalyzed by the WT *E. coli* PNP, only giving rise to the formation of the respective hypothetical furanosides **35a** and **35b** that spontaneously isomerize into the β-D-ribopyranosides **36a** and **36b** in 27 and 8% yield, respectively, according to HPLC analysis (Figure 11) (for the HPLC and mass spectrometry data, see the Experimental Section).

The amorphous N2-(β-D-ribopyranosyl)-2-aminobenzoxazole (**36a**) (IUPAC name: (2*R*,3*S*,4*R*,5*R*)-2-(benzo[d]oxazol-2-ylamino)-tetrahydro-2*H*-pyran-3,4,5-triol) was obtained after column chromatography on reversed-phase silica gel in 25% yield of approximately 93% purity (HPLC). A careful analysis of its ^{1}H and ^{13}C NMR spectra [including (^{1}H,^{1}H) and (^{1}H,^{13}C) 2D COSY, HSQC, HMBC, and NOE spectra—see the Supporting Information, NMR data for compounds **36a** (pages 8–10) and **36b** (pages 11–13)] allowed us to suggest the unexpected structure **36a**, the β-D-ribopyranose fragment of which is attached to the exocyclic amino group. This assignment is based on 1) the presence of one hydrogen atom attached to the exocyclic amino group manifesting strong coupling with the anomeric proton (9.3 Hz, *trans* arrangement), 2) the H1′,H2′ coupling constant of $J = 9.14$ Hz, which is characteristic for the *trans* arrangement of the vicinal protons of the pyranose ring (the H1′,H2′ torsion angle of the pyranose ring of compound **36a** in the most populated $^{4'}C_{1'}$ conformation (see the Experimental Section) correlates well with this coupling constant (compare with data for similar β-D-ribopyranosyl amines[53,54])], 3) the C4′ hydroxyl proton resonance, which appears as a doublet pointing to the coupling with the C4′ vicinal pyranose proton rather than with the C5′ protons of the furanose isomer **35a**, 4) cross peaks of the 4′-OH proton ($\delta = 4.70$ ppm) with the C3′ ($\delta = 71.11$ ppm), C4′ ($\delta = 67.38$ ppm), and C5′ ($\delta = 64.61$ ppm) atoms (see the Supporting Information, Figure 5-E). The ^{13}C HMBC spectrum of compound **36a** (pentopyranose fragment, Supporting Information, page 10) gives further support for the pyranose structure.

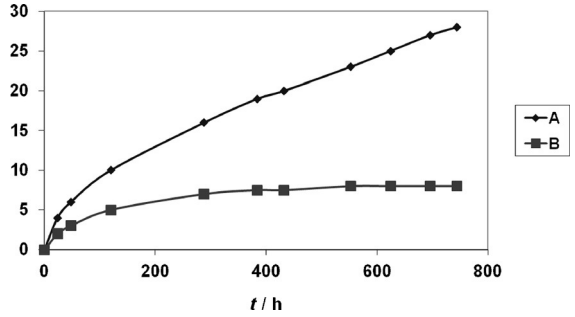

Figure 11. Progress of the synthesis of the ribonucleoside **36a** (A) versus the 2′-deoxyribo **36b** (B) (in [%], ordinate) of 2-amino-1,3-benzoxazole by using the WT *E. coli* PNP (HPLC analysis) (no glycoside formation was observed in the reactions catalyzed by the Ser90Ala mutant enzyme). Reaction conditions: see the Experimental Section.

The 2′-deoxyribonucleoside **36b** of ^{NH_2}BO was formed in 8% yield (HPLC) and was characterized by high-resolution mass spectrometry (see the Experimental Section). Chromatographic purification by using reversed-phase silica gel gave an amorphous product of approximately 90% purity (NMR data, compound is not stable) The detailed analysis of this compound by NMR spectroscopy showed close structural similarity with the riboside **36a** (see the Experimental Section, as well as the spectra in the Supporting Information). The ^{1}H NMR spectrum of the 2′-deoxyribopyranoside **36b** agrees satisfactorily with those of the ribopyranoside **36a** within a range of the resonance signals of aglycone as well as the resonance signals for H1′ [i.e., $\delta = 5.0$ (dt, $^3J(H1',NH) = {}^3J(H1',H2'\alpha) = 9.8$, $^3J(H1',H2'\beta) = 2.2$ Hz)] and H3′ [i.e., $\delta = 3.73$ (dd, $^3J(H3',OH) = 5.6$, $^3J(H3',H2') = 10$, $^3J(H3',H2'\beta) = 4.1$, $^3J(H3',H4') < 1$ Hz)].

It appears to be reasonable that an enzymatic transformation of ^{NH_2}BI and ^{NH_2}BO into the corresponding nucleosides is predominantly realized through the interaction of the Asp204 at the catalytic site of the wild-type PNP with the endocyclic nitrogen atom. In the case of the ^{NH_2}BI ribosylation, an involvement of the Ser90 side chain in the binding resulted in perceptible enhancement of the reaction rate versus the reaction catalyzed by the Ser90Ala mutant enzyme (Figure 10). The principal difference between the ^{NH_2}BI and ^{NH_2}BO glycosylation rates and the structures of the glycosides formed consists in the spatial arrangement of the productive complexes that is suitable electronically for the glycosyl bond formation between the endocyclic nitrogen atom of ^{NH_2}BI (**19** where X = –NH···HO of the Ser90 side chain) and the C1 atom of pentofuranose-1-phosphate on the one hand, whereas the involvement of the exocyclic C2 nitrogen atom (**33**⇄**34**) in the glycosyl bond formation is the only possibility in the ^{NH_2}BO glycosylation on the other. It is noteworthy that from the viewpoint of the electron-

ic structures of the hydrogen-bonded molecules of ^{NH_2}BO (**33**⇄**34**) and ^{NH_2}BS (**33**⇄**34** with a sulphur atom instead an oxygen atom) the glycosylation of the exocyclic nitrogen atom of the latter is not forbidden. However, the binding of ^{NH_2}BS at the catalytic site of the wild-type PNP apparently gives rise to an architecture that is not compatible with the glycosyl bond formation owing to the remarkable dimensional differences of ^{NH_2}BS and ^{NH_2}BO (Figure 12).

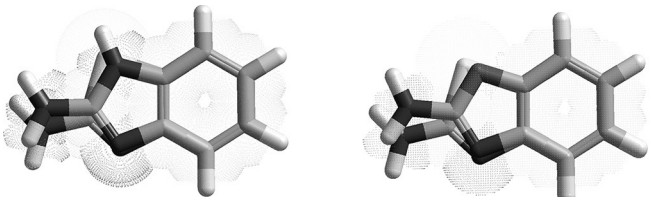

Figure 12. Geometry optimization by ab initio calculations (6-31G**, basis set of parameters, HyperChem 8.1) of 2-aminobenzimidazole (**19a**, left), 2-aminobenzoxazole (**21a**, right), and 2-aminobenzthiazole (**20a**) and overlay of six-membered rings of selected pairs of bases.

It is obvious that the β-D-furanosides **35a** and **35b** are the primary products of the PNP-catalyzed reactions, which isomerize stereospecifically into the β-D-pyranosides **36a** and **36b**. The non-enzymatic spontaneous isomerization of the furanosides **35** into the pyranosides **36** may occur either similar to those described by Montgomery and Thomas[53] and Marquez et al.[54] for relevant β-D-ribofuranosyl amines, or through the tautomeric structure with the intermediary exocyclic double bond (R–N=C2–N1H) and a sp3-hybridized N1 atom followed by the Amadori-like rearrangement reaction accompanied by the enlargement of the ribose ring (see reference [55], for a review see reference [56]).

Conclusion

The substrate properties of a wide range of challenging heterocyclic bases for the recombinant wild-type *E. coli* PNP versus the Ser90Ala mutant were studied to evaluate the mechanism of substrate recognition by PNP and the role of various electronic and structural features in this process. The hypothesis[1] regarding an important role of the Ser90 residue in the recognition of 8-aza-7-deazapurines was confirmed by studying the transribosylation rate (uridine and *E. coli* UP for an in situ Rib-1P generation) and kinetics (co-substrate Rib-1P) of allopurinol (**3**), hypoxanthine, and 5-aza-7-deazaguanine (**8**) as well as by the electronic structure analysis (ab initio calculations and HOMO, LUMO, and HOMO–LUMO gap) of the bases. Replacement of Ser90 with L-alanine gives rise to a dramatic loss of the catalytic activity of the Ser90Ala mutant PNP in the Allo-Rib synthesis.

The substrate activity of 8-aza-7-deaza-2-fluoro-6-methylthiopurine (**5**), 8-aza-7-deaza-2,6-diaminopurine (**6**), and 6-amino-8-aza-7-deaza-2-fluoropurine (**7**) was studied and it was unexpectedly found that the former base **5** is not recognized by the *E. coli* PNP, whereas the two other analogues are excellent substrates in the enzymatic trans-2′-deoxyribosylation (thymidine and *E. coli* TP + *E. coli* PNP) and 2′-deoxyribosylation (dRib-1P and *E. coli* PNP). A good correlation of the E_{LUMO} value and the substrate activity of 8-aza-7-deazapurines was found.

The five-membered rings of 8-amino-7-thiaadenine (**11**) and *N*-(1,3,4-thiadiazol-2-yl)cyanamide (**26**) revealed close similarity, however, the former devoid of substrate activity for both PNPs studied, whereas the latter was found to be a substrate towards mammalian and bacterial PNPs.[41,42] Apparently, the cyanamide function is a major cause of the unusual substrate activity of the base **26** and, therefore, purine analogues (and more structurally distant heterocycles!) containing a cyanamide group are of interest to study their substrate properties.

The reduction of the inosine affinity on going from the WT *E. coli* PNP to the Ser90Ala mutant (Table 2), on the one hand, and a similar weak inhibition of the inosine phosphorolysis by 9-deazaxanthine (**15**) and its 2′-deoxyriboside **17** points to the perceptible role of the Ser90 side chain—N9 interaction in the substrate/inhibitor binding in the *E. coli* PNP catalytic site.

The study of an enzymatic glycosylation of 1,3-benzimidazole (**19**), 1,3-benzothiazole (**20**), and 1,3-benzoxazole (**21**) as well as their 2-amino derivatives **19a**–**21a** revealed that 1) BI is an excellent substrate for both enzymes, 2) ^{NH_2}BI, unlike 8-amino-7-thiapurine (**11**), shows satisfactory and poor substrate activities for the wild-type and mutant PNP, respectively, 3) BS, ^{NH_2}BS (like 8-amino-7-thiapurine (**11**)), and BO are no substrates of both PNPs, 4) ^{NH_2}BO is a very poor substrate only for the wild-type PNP in the reactions of trans-ribosylation and trans-2′-deoxyribosylation, giving rise initially to the respective exocyclic nitrogen atom glycofuranosides **35a** and **35b** that spontaneously isomerize into the β-D-ribopyranosides **36a** and **36b**. Noteworthy, after reaching the maximum conversion of BI and ^{NH_2}BI into their N1-2′-deoxyribosides, a gradual decrease of the concentration of compounds **31b** and **32b** under a further maintaining the reaction mixture was observed only in the case of the wild-type enzyme pointing to dephosphorylation of the intermediate dRib-1P that is likely caused by the participation of the Ser90 residue.

In general, substrate activity of natural purines and their analogues for PNPs is determined by the interplay of various electronic and structural features of heterocyclic bases that affect the interactions with different amino acid residues at the catalytic site. One of the features, for example, the nature of five-membered ring substituent(s), can play a decisive role in the manifestation of substrate properties. Understanding the role of separate feature in the enzymatic synthesis is very important for the design of new heterocycles with the aim of turning them into potentially biologically important nucleosides.

Experimental Section

General methods and material: All chemicals and solvents were of laboratory grade as obtained from commercial suppliers and were used without further purification. TLC was performed on TLC aluminum sheets covered with silica gel 60 F254. UV/Vis spectra were recorded with a Carry 100 spectrometer (Varian, USA). NMR

spectra were recorded at Brucker Avance 500-DRX and 700-DRX spectrometers (Bruker, Germany). Chemical shifts (δ) are given in [ppm]. J values are given in [Hz]. For NMR spectra recorded in [D_6]DMSO, the chemical shift of the solvent peak was set to 2.50 ppm for ^{1}H NMR and to 40.03 ppm for ^{13}C NMR. Mass spectra were measured on Agilent 6224, ESI-TOF, LC/MS (USA) in positive ion mode (ESI), LCQ Fleet ion trap mass spectrometer (Thermo Electron, USA) in 80% acetonitrile. For the high-resolution mass spectrometry results of synthesized benzimidazole nucleosides see Table 6. HPLC system: A) HPLC COMPACT Pump 2050 with a Lambda 1010 UV detector (BISCHOFF Chromatography, Germany), NucleosilC$_{18}$ column, 150×4.6 mm^2, 5 μm, isocratic elution, 1 mL min^{-1}, 5% acetonitrile in 0.1% trifluoroacetic acid TFA/H_2O, v/v; detection at λ0260 nm; B) Waters system (Waters 1525, detector 2487, Breeze 2; USA), MZ PerfectSil 100 ODS-3, 5 μm, 150×4.6 mm^2 column, by using 5% aqueous methanol as the eluent at the wavelength of λ=254 nm, see also in the description of the experiments; C) Waters system by using column Nova Pack C18, 4.6×150 mm^2, 4 μm, detection at λ=280 nm, gradient elution, 1 mL min^{-1}: eluent A: 0.2% TFA/water, eluent B: 70% CH_3CN in 0.1% TFA/water, gradient 0–70% B over 20 min. Flash column chromatography was carry out on silica gel 60, 35–70 μm (Merck, USA).

Table 6. Data of the HR mass spectrometry experiments of the benzimidazole nucleosides.

Starting base	$[M+H]^+$ (calcd)	Nucleoside synthesized	$[M+H]^+$ (calcd)
19	119.0595 (119.0609)	Rib-BI	251.0998 (251.1032)
		dRib-BI	235.1074 (235.1074)
19a	134.0502 (134.0718)	Rib-^{NH_2}BI	266.0716 (266.1141)
		dRib-^{NH_2}BI	250.1180 (250.1192)
21a	135.0543 (135.0540)	Rib-^{NH_2}BO	267.0946 (267.0945)
		dRib-^{NH_2}BO	251.1023 (251.1032)

The following recombinant *E. coli* enzymes[16] were used in the present study: UP, specific activity 100 units per mg, 9 mg per mL, and TP, a solution in 5 mM potassium phosphate buffer (pH 7.0) with an activity of 195 U mL^{-1}, PNP (the product of the *deoD* gene, EC 2.4.2.1) specific activity 54 units per mg, 17 mg per mL. A solution in 20 mM Tris HCl buffer (pH 7.5) with an activity of 918 U mL^{-1} was used in the kinetic experiments and the synthesis of nucleosides **36a** and **36b**.

The preparation of the Ser90Ala *E. coli* PNP (specific activity 1.2 μmol min^{-1} mg^{-1} of protein) is described in the Supporting Information.

α-D-Ribofuranose-1-phosphate (barium salt): In the present synthesis, uridine and *E. coli* UP were used instead of inosine and PNP from rat liver and xanthine oxidase originally described by Kalckar.[57,58]

Uridine (4 g, 16.4 mmol) was dissolved in potassium/phosphate buffer (0.1 M, 330 mL, pH 7.0). UP (25 μL, 56 U) was added and the reaction mixture was kept at 50 °C for three days. After that time HPLC analysis (method A) indicated that about 34% of the uridine were phosphorolyzed. The reaction mixture was cooled to room temperature, precipitated uracil was filtered off, and concentrated ammonia (25% by weight, 110 mL) was added to the filtrate followed by an aqueous solution (80 mL) containing ammonia chloride (17.5 g, 325 mmol) and magnesium chloride (10.1 g of decahydrate, 36.7 mmol). The mixture was kept at 4 °C overnight and was then filtrated. The reaction mixture was evaporated to 300 mL and concentrated ammonia (30 mL), a water solution of barium acetate (20 mL, 4.3 g, 16.8 mmol), and ethanol (300 mL) were added. After one day at 4 °C, precipitated α-D-ribofuranose-1-phoshate (barium salt) was filtered off, washed with ethanol, and dried in vacuum under P_2O_5. Yield: 1.86 g (5.1 mmol, 31%). ^{1}H NMR (700 MHz, D_2O): δ=5.60 (dd, $^3J(H_1,H_2)$=6.5, $^3J(H_1,^{31}P)$=4.1 Hz, 1H; H_1), 4.20–4.27 (m, 1H; H_4), 4.09 (dd, $^3J(H_2,H_3)$=3.9, $^3J(H_2,H_1)$=6.5 Hz, 1H; H_2), 4.02 (dd, $^3J(H_3,H_4)$=6.1, $^3J(H_3,H_2)$=3.9 Hz, 1H; H_3), 3.74 (dd, $^3J(H_4,H_5)$=3.3, $^2J(H_{5\alpha},H_{5\beta})$=12.4 Hz, 1H; $H_{5\alpha}$), 3.62 ppm (dd, $^3J(H_{5\alpha},H_4)$=5.2 Hz, 1H; $H_{5\beta}$); ^{13}C NMR (176 MHz, D_2O): δ=97.26 (C1), 84.34 (C4), 71.64 (C2), 69.84 (C3), 61.56 ppm (C5).

2-Deoxy-α-D-ribofuranose-1-phosphate (barium salt): Thymidine (1.3 g, 5.4 mmol) was dissolved in potassium/phosphate buffer (0.5 M, 15 mL, pH 7.4). TP (200 μL, 39 U) was added and the reaction mixture was kept at 50 °C overnight. After that time HPLC analysis (method A) indicated that about 80% of the thymidine were phosphorolyzed. The reaction mixture was cooled to room temperature, precipitated thymine was filtered off, and concentrated ammonia (25% by weight, 5 mL) was added to the filtrate followed by an aqueous solution (50 mL) containing ammonia chloride (4 g, 74.8 mmol) and magnesium chloride (1.7 g of hexahydrate, 8.4 mmol). The mixture was kept in a freezer at 4 °C for 3 h and was then filtrated. To the filtrate, barium acetate (1.4 g, 5.5 mmol) in water (20 mL) and ethanol (270 mL) were added. After 24 h in the freezer at 4 °C, precipitated 2-deoxy-α-D-ribofuranose-1-phoshate (barium salt) was filtered off, washed with ethanol, and dried in stream of warm air (about 40 °C). Yield: 0.70 g (37%). ^{1}H NMR (500 MHz, D_2O with methanol as an internal standard): δ=5.77 (t, $^3J(H_1,H_2)$=5.2, $^3J(H_1,^{31}P)$=5.2 Hz, 1H; H_1), 4.26–4.19 (br m, 2H; H_3, H_4), 3.72 (dd, $^3J(H_{5\alpha},H_4)$=2.7, $^2J(H_{5\alpha},H_{5\beta})$=12.0 Hz, 1H; $H_{5\alpha}$); 3.58 (dd, $^3J(H_{5\beta},H_4)$=5.5, $^2J(H_{5\beta},H_{5\alpha})$=12.0 Hz, 1H; $H_{5\beta}$), 2.36 (dt, $^3J(H_{2'\alpha},H_{1'})$=$^3J(H_{2'\alpha},H_{3'})$=5.30, $^2J(H_{2''\alpha},H_{2\beta})$=14.75 Hz, 1H; $H_{2'\alpha}$), 2.06 ppm (d, $^3J(H_{2'\beta},H_{1'})$=$^3J(H_{2'\beta},H_{3'})$<0.7, $^2J(H_{2'\alpha},H_{2\beta})$=14.2 Hz, 1H; $H_{2'\beta}$); ^{13}C NMR (126 MHz, D_2O): δ=99.55 (C1), 86.17 (C4), 71.19 (C3), 61.83 (C5), 41.67 ppm (C2); ^{31}P NMR (202 MHz, D_2O): δ=19.03 ppm (d, $J(^{31}P,H_1)$=5.5 Hz); MS (ESI, negative ion mode): *m/z* calcd for $C_5H_{10}O_7P_1$: 213.02; found: 213.2 [$M^+-Ba^{2+}+H$]

Kinetic analysis of the ribosylation of hypoxanthine, allopurinol (3), and 5-aza-7-deazaguanine (8) catalyzed by the WT and Ser90Ala mutant *E. coli* PNPs: Each reaction mixture (0.5 mL, pH 7.0) contained a) hypoxanthine [from 0.005 to 1.2 mM for the wild-type enzyme (final concentration in the reaction mixture 0.255 mg L^{-1}) or from 0.2 to 20 mM for the Ser90Ala mutant (2.4 mg L^{-1})], b) allopurinol [from 0.02 to 4 mM for both enzymes, the WT *E. coli* PNP (2.4 mg L^{-1}) or the mutant PNP (6 mg L^{-1})], or c) 5-aza-7-deazaguanine [from 0.01 to 1.2 mM for both enzymes, the WT *E. coli* PNP (0.255 mg L^{-1}) or the mutant (6 mg L^{-1})], d) inosine [from 0.005 to 1.2 mM for the wild-type enzyme (0.255 mg L^{-1}) or from 0.5 to 50 mM for the Ser90Ala mutant (2.4 mg L^{-1})], e) 2 mM α-D-ribofuranose-1-phosphate (barium salt) or potassium phosphate.

For each experiment, sixteen reaction mixtures were prepared. The reaction was performed at room temperature for various times (from one minute to one day), according to the rate of nucleoside formation. The concentrations of the substrate and the product were determined by isocratic high-performance liquid chromatography (method B). The kinetic parameters were determined by nonlinear regression analysis by using the SciDAVis software v0.2.4 (Data Visualization Platform, SciDAVis; http://sourceforge.net/projects/scidavis/) Then the average value of the constants for three experiments was calculated. The k_{cat} values (turnover number)

were calculated per whole enzyme by using a PNP mass of 156 kDa.[16]

Kinetic analysis of the inhibitory activities of the 9-deazapurines 15 and 16 and their nucleosides 17 and 18: In preliminary experiments the rate of inosine phosphorolysis in the presence or absence of the tested compounds was compared. Reaction conditions: 100 mM potassium/phosphate buffer (pH 7.3), 0.75 mM inosine, approximately 0.75 mM inhibitor, 0.005 U of PNP per μmol of inosine. After being kept at 20 °C for 10 min a drop of 1 M HCl was added and the reaction mixture was analyzed by HPLC (method A).

Based on preliminary data, phoshorolysis of inosine in the range of concentrations of 35–105 μM was analyzed in the presence of 0, 11, 14, and 18 μM of 9-deaza-9-iodoxanthine (**16**), 100 mM potassium/phosphate buffer (pH 7.3), 2.5 U L^{-1} (0.93·10–3 mg L^{-1}) of PNP, progress of the phosphorolysis was monitored by UV at $\lambda =$ 248 nm ($\Delta\varepsilon = 3160\ M^{-1}\,cm^{-1}$).

8-Aza-7-deaza-9-(2-deoxy-β-D-ribofuranosyl)-2,6-diaminopurine (6a)

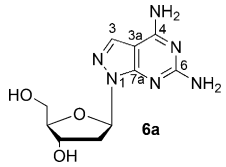

Chemical formula: $C_{10}H_{14}N_6O_3$
Exact mass: 266.11

6a

To a solution of thymidine (200 mg, 0.83 mmol) in potassium/phosphate buffer (0.2 M, pH 7.4, 10 mL) was added TP (40 μL, 7.8 U) and the reaction mixture was stirred at 40 °C for 1 h resulting in almost complete phosphorolysis of thymidine according to HPLC analysis (method A). PNP (120 μL, 13 U) was added to the reaction mixture and then the heterocyclic base **6**[22a] [solution of 70 mg (0.47 mmol) in DMSO (2 mL)] was added dropwise to the mixture, which was stirred at 40 °C and the formation of the nucleoside **6a** was monitored by HPLC (method A): R_t values: thymidine = 4.6, thymine = 3.2, compound **6** = 6.1, compound **6a** = 3.7 min. After 18 h, very small quantity of the starting base remained in the reaction mixture and the precipitate consisting of thymine and the desired nucleoside was formed. It was filtered off, dissolved in ethanol, absorbed on silica gel (3 mL), and put on the top of the silica gel column (3×15 cm^2), which was then eluted with chloroform/methanol (8:1, v/v) to afford the nucleoside **6a** as a white powder (90 mg, 71%). ^{1}H NMR (500 MHz, [D$_6$]DMSO): $\delta = 7.83$ (s, 1H; H$_3$), 7.20 (brs, 2H; NH$_2$), 6.31 (t, $^3J(H_{1'},H_{2'\alpha}) = {}^3J(H_{1'},H_{2'\beta}) = 6.6$ Hz, 1H; H$_{1'}$), 6.14 (brs, 2H; NH$_2$), 5.20 (d, ^3J(OH,H$_{3'}$) = 4.3 Hz; 1H; 3′-OH), 4.98–4.72 (brs, 1H; 5′-OH), 4.34 (d of brt, $^3J(H_{3'},H_{2'a}) = 6.3$, $^3J(H_{3'},H_{2'b}) = 3.6$, $^3J(H_{3'},H_{4'}) = 3.6$ Hz, 1H; H$_{3'}$), 3.74 (dt, $^3J(H_{4'},H_{5'}) = 5.4$, $^3J(H_{4'},H_{3'}) = 3.1$ Hz, 1H; H$_{4'}$), 3.46 (dd, $^2J(H_{5'\alpha},H_{5'\beta}) = 11.5$, $^3J(H_{5'\alpha},H_{4'}) =$ 5.5 Hz, 1H; H$_{5'\alpha}$), 3.36 (dd, $^3J(H_{5'\beta},H_{4'}) = 5.5$ Hz; 1H; H$_{5'\beta}$), 2.71 (dt , $^2J(H_{2'\alpha},H_{2'\beta}) = 12.9$, $^3J(H_{1'},H_{2'\alpha}) = {}^3J(H_{2'\alpha},H_{3'}) = 6.3$ Hz, 1H; H$_{2'\alpha}$), 2.12 ppm (ddd, $^2J(H_{2'\beta},H_{2'\alpha}) = 13.0$, $^3J(H_{2'\beta},H_{1'}) = 6.6$, $^3J(H_{2'\beta},H_{3'}) =$ 3.6 Hz, 1H; H$_{2'\beta}$); the resonance signal of H$_{5'\beta}$ is overlapped by the HOD signal; ^{13}C NMR (126 MHz, D$_2$O) (purine numbering is italicized): $\delta = 162.61$ (C4/*C6*), 158.53 (C7a/*C4*), 156.88 (C6/*C2*), 133.94 (C3/*C7*), 95.93 (C3a/*C5*), 87.56 (C4′), 84.01 (C1′), 71.74 (C3′), 63.00 (C5′), 38.24 ppm (C2′), the NMR spectrum is in a fair agreement with data published by He and Seela;[59] UV/Vis (H$_2$O): λ_{max} (ε) = 274 (7100), 257 (6200) (pH 7), 274 (7400), 257 (6900) (pH > 10), 256 (8100 mol^{-1} m^3 cm^{-1}), and shoulder at 280 nm (pH < 4); λ_{min} (ε) = 263 (6200), 239 (3500) at pH 7, 263 (6500), 239 (6900) at pH > 10, 239 nm (4900 mol^{-1} m^3 cm^{-1}) (pH < 4); MS (Thermo electron; positive ion mode): *m/z* (%) calcd for $C_{10}H_{14}O_3N_6$: 266.11; found: 268.1 (10) [M^++2H], 267.1 (100) [M^++H], 151.2 (23), [$C_5H_7N_6^+$ (base+H$^+$)], 113.2 (2), 60.1 (6).

6-Amino-8-aza-7-deaza-2-fluoropurine (7)

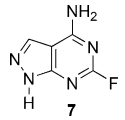

Chemical formula: $C_5H_4FN_5$
Exact mass: 153.05

7

To a suspension of 4,6-diaminopyrazolo[3,4-*d*]pyrimidine (0.55 g, 4.23 mmol) in HF/pyridine (70%, 5 mL) cooled at −11 °C with an ice/salt bath was added an aqueous solution of KNO_2 (0.49 g, 5.76 mmol) in water (0.2 mL) over one hour. After the addition, the mixture was stirred for another two hours with the temperature increasing from −11 to 6 °C. The mixture was poured into an ice-cooled calcium carbonate mixture and stored overnight. Methanol (500 mL) was used to extract the product from the mixture. The product was further purified by flash chromatography and a colorless solid (120 mg, 21%) was received. R_f (CH_2Cl_2/CH_3OH, 9:1): 0.31; elemental analysis calcd for $C_5H_4FN_5$ (153): C 39.22, H 2.63, N 45.74; found: C 38.96, H 2.50, N 45.30.

6-Amino-8-aza-7-deaza-9-(2-deoxy-β-D-ribofuranosyl)-2-fluoropurine (7a)

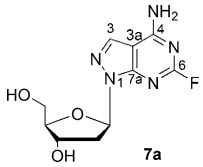

Chemical formula: $C_{10}H_{12}FN_5O_3$
Exact mass: 269.0924
Molecular weight: 269.234

7a

2-Deoxy-α-D-ribofuranose-1-phoshate (barium salt) (14 mg, 40.1 μmol) was dissolved in Tris·HCl buffer (20 mM, 5 mL, pH 7.2). PNP (20 μL, 2.2 U) was added and 2-fluoro-6-amino-8-aza-7-deazapurine (**7**) (3 mg, 19.6 μmol) in DMSO (0.5 mL) was added dropwise with stirring. The progress of the reaction was monitored by HPLC (method A). R_t values: base **7** = 6.2, nucleoside **7a** = 12.0 min). After 2 h, complete transformation of the base **7** into the nucleoside **7a** was observed according to HPLC. The reaction mixture was evaporated to dryness, the residue was dissolved in ethanol, absorbed on silica gel (0.5 mL), and put on the top of the silica gel column (1.0×10 cm^2), which was then eluted with chloroform/methanol (10:1, v/v) to afford the nucleoside **7a** as a white powder (5 mg, 95%). ^{1}H NMR (500 MHz, D$_2$O with CH_3CN as an internal standard): $\delta = 7.44$ (s, 1H; H$_3$), 5.84 (t, $^3J(H_{1'},H_{2'\alpha}) = {}^3J(H_{1'},H_{2'\beta}) = 6.6$ Hz, 1H; H$_{1'}$), 3.99 (dt, $^3J(H_{3'},H_{2'\alpha}) = 6.5$, $^3J(H_{3'},H_{2'\beta}) = 3.9$, $^3J(H_{3'},H_{4'}) = 3.9$ Hz, 1H; H$_{3'}$), 3.43 (dt, $^3J(H_{4'},H_{3'}) = {}^3J(H_{4'},H_{5'\alpha}) = 3.9$, $^3J(H_{4'},H_{5'\beta}) = 6.9$ Hz, 1H; H$_{4'}$), 3.11 (dd, $^3J(H_{5'\alpha,4'}) = 4.1$, $^2J(H_{5'\alpha},H_{5'\beta}) = 12.2$ Hz, 1H; H$_{5'\alpha}$), 3.00 (dd, $^3J(H_{5'\beta,4'}) = 6.0$, $^2J(H_{5'\beta},H_{5'\alpha}) = 12.3$ Hz, 1H; H$_{5'\beta}$), 2.29 (dt, $^3J(H_{2'\alpha,1'}) =$ $^3J(H_{2'\alpha,3'}) = 6.4$, $^2J(H_{2'\alpha},H_{2'\beta}) = 13.9$ Hz; 1H, H$_{2'\alpha}$), 1.83 ppm (ddd, $^3J(H_{2'\beta,1'}) = 6.8$, $^3J(H_{2'\beta,3'}) = 4.1$, $^2J(H_{2'\beta},H_{2'\alpha}) = 14.1$ Hz, 1H; 2′-H$_\beta$); ^{13}C NMR (126 MHz) (purine numbering is italicized): $\delta = 162.43$ (d, $^1J(^{13}C_6,^{19}F) = 212.88$ Hz; C6/*C2*), 160.47 (d, $^3J(^{13}C_{7a},^{19}F) = 20.80$ Hz, C7a/*C4*), 155.45 (d, $^3J(^{13}C_4,^{19}F) = 18.96$ Hz; C4/*C6*), 135.11 (C3/*C7*), 119.50 (Me-*C*=N), 99.90 (C3a/*C5*), 87.23 (C4′), 84.86 (C1′), 71.64 (C3′), 63.50 (C5′), 39.11 (C2′), 1.42 ppm (CH_3-C=N); UV/Vis (H$_2$O): λ_{max} = 264 (pH 7), 263 (pH < 4), 265 nm (pH > 10); $\lambda_{min} = 237$ (pH 7, pH < 4), 241 nm (pH > 10); MS (ESI, positive ion mode): *m/z* (%) calcd for $C_{10}H_{12}FO_3N_5$: 269.09; found: 270.0 (100) [M+H$^+$], 251.2 (40), [M^+ −H$_2$O], 154.1 (48) [$C_5H_5FN_5^+$ (base+H$^+$)], 104.1 (59).

2-Amino-1-(2-deoxy-β-D-ribofuranosyl)-1,3-benzimidazole (32b)

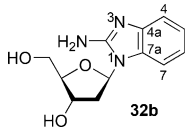

Chemical formula: $C_{12}H_{15}N_3O_3$
Exact mass: 249.1113
Molecular weight: 249.267

A mixture of 2-amino-1,3-benzimidazole (**19a**) (0.13 g, 1 mmol), 2′-deoxyguanosine (dG, 0.4 g, 1.5 mmol), and PNP (54 IU) in potassium/phosphate buffer (20 mM, 15 mL, pH 7.0) was gentle stirred at 50 °C for 30 h, monitoring the formation of the nucleoside **32b** by TLC (UV detection, elution with the CH_2Cl_2/EtOH/AcOH, 85:10:5 (v/v/v), R_f: **15a** = 0.25; dG = 0.02, **15** = 0.15 min). The reaction mixture was evaporated to dryness; the residue was dissolved in dry EtOH, one tee spoon of SiO_2 was added to the solution, and the mixture was evaporated to dryness. The SiO_2 with the product was placed on the top of the SiO_2 column [20×180 mm², prepared in CH_2Cl_2(MeOH (95:5 v/v)] that was eluted with a linear MeOH gradient 5→20% (v) in CH_2Cl_2 (2×1000 mL). The fractions containing the nucleoside **32b** were pooled and evaporated to give the TLC- and HPLC-pure product (0.22 g, 91%), a portion of which was crystallized from a EtOH/ether mixture. M.p. 179–184 °C [measured on the WRS-2 (BestScope, China)]; ^{1}H NMR (500 MHz, [D$_6$]DMSO): δ = 7.28 (d, $^3J(H_4,H_5)$/(H_7,H_6) = 7.77 Hz, 1H; H_4/H_7), 7.12 (d, $^3J(H_7,H_6)$/(H_4,H_5) = 7.72 Hz, 1H; H_4/H_7), 6.96 (dt, $^3J(H_5,H_4)$/(H_6,H_5) = $^3J(H_5,H_6)$/(H_6,H_7) = 7.60, $^4J(H_5,H_7)$/(H_6,H_4) = 0.90 Hz, 1H; H_6/H_7), 6.87 (dt, $^3J(H_6,H_5)$/(H_5,H_4) = $^3J(H_6,H_7)$/(H_5,H_6) = 7.56, $^4J(H_5,H_7)$/(H_6,H_4) = 1.02 Hz, 1H; H_6/H_7), 6.51 (s, 2H; NH_2), 6.23 (dd, $^3J(H_{1'},H_{2'\alpha})$ = 8.80, $^3J(H_{1'},H_{2'\beta})$ = 6.15 Hz, 1H; $H_{1'}$), 5.30 (d, $^3J(OH,H_{3'})$ = 4.17 Hz, 1H; 3′-OH) 5.29 (t, $^3J(OH,H_{5'\alpha})$ = $^3J(OH,H_{5'\beta})$ = 4.88 Hz, 1H; 5′-OH), ca. 2.5 ($H_{2'\alpha}$, overlapped by the [D$_6$]DMSO resonance), 2.02 (ddd, $^3J(H_{2'\beta},H_{1'})$ = 6.12, $^3J(H_{2'\beta},H_{3'})$ = 2.25, $^2J(H_{2'\beta},H_{2'\alpha})$ = 13.21 Hz, 1H; $H_{2'\beta}$), 4.39 (br dt, $^3J(H_{3'},OH)$ = 4.20, $^3J(H_{3'},H_{4'})$ = 3.0, $^3J(H_{3'},H_{2'\beta'})$ = 2.50 Hz, 1H; $H_{3'}$), 3.82 (dt, $^3J(H_{4'},H_{3'})$ = 3.00, $^3J(H_{4'},H_{5'\alpha})$ = $^3J(H_{4'},H_{5'\beta})$ = 3.16 Hz, 1H; $H_{4'}$), 3.67 ppm (dt, $^3J(H_{5'\alpha},OH)$ = 4.58, $^3J(H_{5'\alpha},H_{4'})$ = $^3J(H_{5'\beta},H_{4'})$ = 3.16 Hz, 2H; $H_{5'\alpha\beta}$); ^{13}C NMR (126 MHz, [D$_6$]DMSO): δ = 154 (C2), 142.83 (C7a), 132.74 (C4a), 120.68 (C7), 118.19 and 114.89 (C4, C5), 108.74 (C6), 86.67 (C4′), 83.53 (C1′), 70.41 (C3′), 61.01 (C5′), 37.86 ppm (C2′); UV/Vis (H_2O): λ_{max} (ε) = 280 (6350), 243 (2000) (pH 7), 282 (6250), 244 (7650) (pH > 10), 280 (6450), 274 nm (7050 mol^{-1} m^3 cm^{-1}) (pH < 4); λ_{min} (ε) = 259 (2000), 235 (5650) (pH 7), 260 (1850) 230 (5500) (pH > 10), 278 (6250), 246 nm (750 mol^{-1} m^3 cm^{-1}) (pH < 4); MS (ESI, positive ion mode): *m/z* (%) calcd for $C_{12}H_{15}O_3N_3$: 249.11; found: 251.2 (9), $[M+2H]^+$, 250.1 (100), $[M+H]^+$, 135.1 (3), $[base+2H]^+$, 134.2 (56) $[base+H]^+$; MS HR (ESI, positive ion mode): *m/z* (%) calcd for $C_{12}H_{15}O_3N_3$: 250.1180 $[M^+ + H]$; found: 250.1192.

N2-(β-D-Ribopyranosyl)-2-amino-1,3-benzoxazole (36a) [IUPAC name: (2*R*,3*R*,4*R*,5*R*)-2-(benzo[*d*]oxazol-2-ylamino)tetrahydro-2*H*-pyran-3,4,5-triol] by transglycosylation of 2-amino-1,3-benzoxazole (21a)

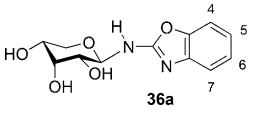

Chemical formula: $C_{12}H_{14}N_2O_5$
Exact mass: 266.0903
Molecular weight: 266.26

A mixture of 2-amino-1,3-benzoxazazole (**21a**) (0.02 g, 2 mmol), uridine (U, 0.366 g, 20 mmol), UP (540 IU, preparation: 9 mg mL^{-1}, 100 U mg^{-1}), and PNP (550.8 IU, preparation: 17 mg mL^{-1}, 54 U mg^{-1}) in potassium phosphate buffer (20 mM, 75 mL, pH 7.0) was incubated at 55 °C for 744 h, monitoring the formation of the nucleoside **36a** by HPLC (method C, R_t: Ura = 2.1, Urd = 2.5, **21a** = 7.0, **36a** = 7.6 min). The reaction mixture was evaporated to 4 mL; and compound **36a** was obtained after preparative HPLC on reversed phase C18 silica gel (20×250 mm²; MZ-preparative, Germany). Compound **36a** was eluted with a linear MeOH gradient 0→20% (v). The fractions containing the nucleoside **36a** were pooled and evaporated to give the desired nucleoside **36a** (0.01 g, purity 93% by HPLC) in 25% yield. For a geometry-optimized structure of nucleoside **36a** by using the PM3 method, see below. ^{1}H NMR (700 MHz, [D$_6$]DMSO, 30 °C): δ = 8.49 (d, $^3J(NH,H_{1'})$ = 9.3 Hz, 1H; NH), 7.38 (d, $^3J(H_4,H_5)$ = 7.9 Hz, 1H; H_4), 7.28 (d, $^3J(H_7,H_6)$ = 7.7 Hz, 1H; H_7), 7.14 (dt, $^3J(H_6,H_5)$ = $^3J(H_6,H_7)$ = 7.7, $^4J(H_6,H_4)$ ≈ 1 Hz, 1H; H_6), 7.01 (dt, $^3J(H_5,H_4)$ = $^3J(H_5,H_6)$ = 7.8, $^4J(H_5,H_7)$ ≈ 1 Hz, 1H; H_5), 5.035 (t, $^3J(H_{1'},NH)$ = $^3J(H_{1'},H_{2'})$ = 9.14 Hz, 1H; $H_{1'}$), 4.85 (d, $^3J(OH,H_{3'})$ = 3.6 Hz, 1H; 3′-OH), 4.77 (d, $^3J(OH,H_{2'})$ = 7.0 Hz, 1H; 2′-OH), 4.69 (d, $^3J(OH,H_{4'})$ = 5.8 Hz, 1H; 4′-OH), 3.93–3.95 (m, $^3J(H_{3'},OH)$ = 3.6, $^3J(H_{3'},H_{2'})$ = 2.8, $^3J(H_{3'},H_{4'})$ ≈ 2 Hz, 1H; $H_{3'}$), 3.53–3.55 (m, $^3J(H_{4'},OH)$ = 5.8, $^3J(H_{4'},H_{5'})$ ≈ 5, $^3J(H_{4'},H_{3'})$ ≈ 2 Hz, 1H; $H_{4'}$), 3.53 (dd, $^2J(H_{5'\alpha},H_{5'\beta})$ = 11.0, $^3J(H_{5'\alpha},H_{4'})$ ≈ 3 Hz, 1H; $H_{5'\alpha}$), 3.47 (dd, $^2J(H_{5'\beta},H_{5'\alpha})$ = 11.0, $^3J(H_{5'\beta},H_{4'})$ ≈ 5 Hz, 1H; $H_{5'\beta}$), 3.40 ppm (td, $^3J(H_{2'},H_{1'})$ = 9.1, $^3J(H_{2'},OH)$ = 7, $^3J(H_{2'},H_{3'})$ = 2.8 Hz, 1H; $H_{2'}$); ^{13}C NMR (176 MHz, [D$_6$]DMSO, 30 °C): δ = 162.42 (C2), 148.35 (C4a), 143.22 (C7a), 124.21 (C6), 121.02 (C5), 116.29 (C7), 109.19 (C4), 81.35 (C1′), 71.27 (C3′), 69.99 (C2′), 67.53 (C4′), 64.73 ppm (C5′); ^{15}N NMR (71 MHz, [D$_6$]DMSO, 30 °C): δ = 84.3 ppm (NH); UV/Vis (H_2O): λ_{max}: 240, 278 nm (pH 7); MS (ESI, positive ion mode): *m/z* (%) calcd for $C_{12}H_{14}O_5N_2$: 267.0945; found: 267.09679 $[M^+ + H]$; calcd for $C_7H_6N_2O^+$: 135.0540; found: 135.05484 [base+H].

N2-(2-Deoxy-β-D-ribopyranosyl)-2-amino-1,3-benzoxazole (36b) [IUPAC name (2*R*,3*R*,4*R*,5*R*)-2-(benzo[*d*]oxazol-2-ylamino)tetrahydro-2*H*-pyran-4,5-diol] by transglycosylation of 2-amino-1,3-benzoxazole (17a)

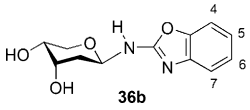

Chemical formula: $C_{12}H_{14}N_2O_4$
Exact mass: 250.0954
Molecular weight: 250.2518

A mixture of 2-amino-1,3-benzoxazazole (**21a**) (0.02 g, 2 mmol), 2′-deoxyuridine (dU, 0.068 g, 4 mmol), UP (246 IU, preparation: 9 mg mL^{-1}, 100 U mg^{-1}), and PNP (149 IU, preparation: 17 mg mL^{-1}, 54 U mg^{-1}) in potassium phosphate buffer (20 mmol, 75 mL, pH 7.0) was incubated at 55 °C for 744 h monitoring the formation of the nucleoside **36b** by HPLC (detection at λ = 280 nm, elution with the CH_3CN/H_2O/TFA 70:30:0.1 (v/v/v), R_t: Ura = 2.1, dU = 2.5, **17a** = 7.0; **33b** = 8.9 min). The reaction mixture was evaporated to 3 mL and compound **36b** was obtained after preparative HPLC on reversed phase C18 silica gel (20×250 mm², MZ-preparative). Nucleoside **36b** was eluted with a linear MeOH gradient 0→20% (v). The fractions containing the nucleoside **36b** were pooled and evaporated to give the HPLC-pure product (0.003 g, 93%) in 8% yield. ^{1}H NMR (700 MHz, [D$_6$]DMSO, 30 °C): δ = 8.62 (d, $^3J(NH,H_{1'})$ = 9.0 Hz, 1H; NH), 7.39 (d, $^3J(H_4,H_5)$ = 7.9 Hz, 1H; H_4), 7.29 (d, $^3J(H_7,H_6)$ = 7.8 Hz, 1H; H_7), 7.15 (dt, $^3J(H_6,H_5)$ = $^3J(H_6,H_7)$ = 7.9 Hz, 1H; H_6), 7.04 (dt, $^3J(H_5,H_4)$ = $^3J(H_5,H_6)$ = 7.7 Hz, 1H; H_5), 5.0 (dt, $^3J(H_{1'},NH)$ = $^3J(H_{1'},H_{2'\alpha})$ = 9.8, $^3J(H_{1'},H_{2'\beta})$ = 2.2 Hz, 1H; $H_{1'}$), 4.81 (d, $^3J(OH,H_{3'})$ = 5.6 Hz, 1H; 3′-OH), 4.48 (d, $^3J(OH,H_{4'})$ = 3.2 Hz, 1H; 4′-OH), ca. 3.73 (overlapped with low field doublet of the H_{5a} resonance; the following coupling constants are obtained from the resonance of vicinal protons and 3′-OH: $^3J(H_{3'},OH)$ = 5.6, $^3J(H_{3'},H_{2'})$ = 10, $^3J(H_{3'},H_{2'\beta})$ = 4.1, $^3J(H_{3'},H_{4'})$ < 1 Hz, 1H; $H_{3'}$), 3.3-3.7 (br m, the follow-

ing coupling constants are obtained from the resonance of vicinal protons and 4′-OH: $^{3}J(H_{4'},OH) = 3.2$, $^{3}J(H_{4'},H_{5'\alpha}) = 2.8$, $^{3}J(H_{4'},H_{5'\beta}) = 1.1$, $^{3}J(H_{4'},H_{3'}) < 1$ Hz, 1H; $H_{4'}$), 3.75 (dd, $^{2}J(H_{5'\alpha},H_{5'\beta}) = 12.0$, $^{3}J(H_{5'\alpha},H_{4'}) =$ 2.8 Hz, 1H; $H_{5'\alpha}$), 3.48 (dd, $^{2}J(H_{5'\beta},H_{5'\alpha}) = 12$, $^{3}J(H_{5'\beta},H_{4'}) = 1.8$ Hz, 1H; $H_{5'\beta}$), 1.92 (td, $^{2}J(H_{2'\alpha},H_{2'\beta}) = 12.4$, $^{3}J(H_{2'\alpha},H_{1'}) = 9.8$, $^{3}J(H_{2'\alpha},H_{3'}) =$ 10.0 Hz, 1H; $H_{2'\alpha}$), 1.76 ppm (td, $^{2}J(H_{2'\beta},H_{2'\alpha}) = 12$, $^{3}J(H_{2'\beta},H_{1'}) = 2.2$, $^{3}J(H_{2'\beta},H_{3'}) = 4.1$ Hz, 1H; $H_{2'\beta}$); ^{13}C NMR (176 MHz, [D$_6$]DMSO, 30 °C): $\delta = 161.50$ (C2), 148.24 (C4a), 143.0 (C7a), 124.18 (C6), 121.05 (C5), 116.31 (C7), 109.15 (C4), 80.33 (C1′), 68.14 (C3′), 66.86 (C4′), 67.66 (C5′), 34.82 ppm (C2′); ^{15}N NMR (71 MHz, [D$_6$][D$_6$]DMSO, 30 °C): $\delta =$ 88.93 ppm (NH); UV/Vis (H_2O): $\lambda_{max} = 270$, 227 nm (pH 7); MS (ESI, positive ion mode): *m/z* (%) calcd for $C_{12}H_{14}O_4N_2$: 251.1032; found: 251.10006 [M^++H], 273.08183 [M^++Na]; calcd for: 135.0540; found: 135.05366 [base+H]$^+$.

Acknowledgements

The authors are thankful to the International Science and Technology Centre (ISIC, http://www.istc.ru, project #B-1640) for the financial support of this work. I.A.M. is deeply thankful to the Alexander von Humboldt-Stiftung (Bonn–Bad-Godesberg, Germany) and the Byelorussian Republican Foundation for Fundamental Research (http://www.fond.bas-net.by, project No. X13MC-027) for partial financial support. We are indebted to Dr. T. A. Balashova (Institute of Bioorganic Chemistry, Moscow) for assistance in the analysis of the NMR spectra of the new nucleosides.

Keywords: ab initio calculations · *escherichia coli* · glycosylation · nucleobases · purine analogues · substrate properties

[1] V. A. Stepchenko, F. Seela, R. S. Esipov, A. I. Miroshnikov, Y. A. Sokolov, I. A. Mikhailopulo, *Syn. Lett.* **2012**, *23*, 1541 – 1545.
[2] E. M. Bennett, C. Li, P. W. Allan, W. B. Parker, S. E. Ealick, *J. Biol. Chem.* **2003**, *278*, 47110 – 47118.
[3] Y. Zhang, W. B. Parker, E. J. Sorscher, S. E. Ealick, *Curr. Topics Med. Chem.* **2005**, *5*, 1259 – 1274.
[4] a) I. A. Mikhailopulo, A. I. Miroshnikov, *Acta Naturae* **2010**, *2*, 38 – 61; b) I. A. Mikhailopulo, A. I. Miroshnikov, *Mendeleev Commun.* **2011**, *21*, 57 – 68.
[5] T. A. Krenitsky, G. B. Elion, R. A. Strelitz, G. H. Hitchings, *J. Biol. Chem.* **1967**, *242*, 2675 – 2682.
[6] M. D. Erion, J. D. Stoeckler, W. C. Guida, R. L. Walter, S. E. Ealick, *Biochemistry* **1997**, *36*, 11735 – 11748.
[7] a) A. Bzowska, E. Kulikowska, D. Shugar, *J. Clin. Pharm. Ther.* **2000**, *88*, 349 – 425; b) A. Bzowska, E. Kulikowska, D. Shugar, *Biochim. Biophys. Acta* **1992**, *1120*, 239 – 247; c) M. R. Sheen, B. K. Kim, R. E. Parks Jr., *Mol. Pharmacol.* **1968**, *4*, 293 – 299; d) B. Wielgus-Kutrowska, E. Kulikowska, J. Wierzchowski, A. Bzowska, D. Shugar, *Eur. J. Biochem.* **1997**, *243*, 408 – 417.
[8] G. Koellner, M. Luic, D. Shugar, W. Saenger, A. Bzowska, *J. Mol. Biol.* **1998**, *280*, 153 – 166.
[9] C. Mao, W. J. Cook, M. Zhou, G. W. Koszalka, T. A. Krenitsky, S. E. Ealick, *Structure* **1997**, *5*, 1373 – 1383.
[10] G. Koellner, A. Bzowska, B. Wielgus-Kutrowska, M. Luic, T. Steiner, W. Saenger, J. Stepinski, *J. Mol. Biol.* **2002**, *315*, 351 – 371.
[11] W. Ye, D. Paul, L. Gao, J. Seckute, R. Sangaiah, K. Jayaraj, Z. Zhang, P. A. Kaminski, S. E. Ealick, A. Gold, L. M. Ball, *PLoS ONE* **2014**, *9*, DOI: 10.1371/journal.pone.0115082.
[12] G. Mikleusevic, Z. Stefanic, M. Narczyk, B. Wielgus-Kutrowska, A. Bzowska, M. Luic, *Biochimie* **2011**, *93*, 1610 – 1622.
[13] a) E. Kulikowska, A. Bzowska, J. Wierzchowski, D. Shugar, *Biochim. Biophys. Acta* **1986**, *874*, 355 – 366; b) A. Bzowska, E. Kulikowska, D. Shugar, *Z. Naturforsch. C* **1990**, *45*, 59 – 70.
[14] W. J. Hennen, C.-H. Wong, *J. Org. Chem.* **1989**, *54*, 4692 – 4695.
[15] J. J. Voegel, M. M. Altorfer, S. A. Benner, *Helv. Chim. Acta* **1993**, *76*, 2061 – 2069.
[16] R. S. Esipov, A. I. Gurevich, D. V. Chuvikovsky, L. A. Chupova, T. I. Muravyova, A. I. Miroshnikov, *Protein Expression Purif.* **2002**, *24*, 56 – 60.
[17] J. Doskocil, A. Holy, *Collect. Czech. Chem. Commun.* **1977**, *42*, 370 – 383, and references therein.
[18] I. Votruba, A. Holy, H. Dvorakova, J. Gunther, D. Hockova, H. Hrebabecky, T. Cihlar, M. Masojidkova, *Collect. Czech. Chem. Commun.* **1994**, *59*, 2303 – 2330.
[19] a) H. Rosemeyer, F. Seela, *J. Org. Chem.* **1987**, *52*, 5136 – 5143; F. Seela, H. Rosemeyer in *Recent Advances in Nucleosides: Chemistry and Chemotherapy* (Ed.: C. K. Chu), Elsevier, Amsterdam, **2002**, pp. 505 – 533.
[20] I. V. Fateev, K. V. Antonov, I. D. Konstantinova, T. I. Muravyova, F. Seela, R. S. Esipov, A. I. Miroshnikov, I. A. Mikhailopulo, *Beilstein J. Org. Chem.* **2014**, *10*, 1657 – 1669.
[21] T. Steiner, *Angew. Chem. Int. Ed.* **2002**, *41*, 48 – 76; *Angew. Chem.* **2002**, *114*, 50 – 80.
[22] A. A. Granovsky, Firefly version 7.1.G, http://classic.chem.msu.su/gran/firefly/index.html.
[23] M. W. Schmidt, K. K. Baldridge, J. A. Boatz, S. T. Elbert, M. S. Gordon, J. H. Jensen, S. Koseki, M. Matsunaga, K. A. Nguyen, S. Su, T. L. Windus, M. Dupuis, *J. Comput. Chem.* **1993**, *14*, 1347 – 1363.
[24] a) F. Seela, K. Xu, *Org. Biomol. Chem.* **2007**, *5*, 3034 – 3045; b) F. Seela, H. Driller, *Helv. Chim. Acta* **1988**, *71*, 757 – 761.
[25] M. Friedkin, *J. Biol. Chem.* **1950**, *184*, 449 – 460.
[26] H. Komatsu, H. Awano, *J. Org. Chem.* **2002**, *67*, 5419 – 5421.
[27] I. A. Mikhailopulo, S. Lapinjoki, Biocatalytic Synthesis of Pharmaceutically Important Nucleosides: Proceedings of the FinMed 2006 (Eds.: S. Sorvari, O. Toldi), Saariselkä, Lapland (Finland), 27 – 31 March, **2006**, ISBN-13: 978-952-99302-4-1, pp. 42 – 51.
[28] J. Roivainen, T. Elizarova, S. Lapinjoki, I. A. Mikhailopulo, R. S. Esipov, A. I. Miroshnikov, *Nucleosides Nucleotides Nucleic Acids* **2007**, *26*, 905 – 909.
[29] I. D. Konstantinova, K. V. Antonov, I. V. Fateev, A. I. Miroshnikov, V. A. Stepchenko, A. V. Baranovsky, I. A. Mikhailopulo, *Synthesis* **2011**, 1555 – 1560.
[30] A. I. Kulikovskiy, R. S. Esipov, A. I. Miroshnikov, I. A. Mikhailopulo, *Collect. Symp. Ser.* **2011**, *12*, 397 – 240.
[31] I. D. Konstantinova, O. M. Selezneva, I. V. Fateev, T. A. Balashova, S. K. Kotovskaya, Z. M. Baskakova, V. N. Charushin, A. V. Baranovsky, A. I. Miroshnikov, J. Balzarini, I. A. Mikhailopulo, *Synthesis* **2013**, 272 – 280.
[32] I. A. Mikhailopulo, *Curr. Org. Chem.* **2007**, *11*, 317 – 335.
[33] I. A. Mikhailopulo, A. I. Zinchenko, S. B. Bokut, N. V. Dudchik, V. N. Barai, E. N. Kalinichenko, H. Rosemeyer, F. Seela, *Biotechnol. Lett.* **1992**, *14*, 885 – 890.
[34] I. A. Mikhailopulo, Z. Kazimierczuk, A. I. Zinchenko, V. N. Barai, V. V. Romanova, L. A. Eroshevskaya, *Nucleic Acids Symp. Ser.* **1994**, *31*, 83.
[35] I. A. Mikhailopulo, Z. Kazimierczuk, A. I. Zinchenko, V. N. Barai, V. V. Romanova, L. A. Eroshevskaya, *Nucleosides Nucleotides* **1995**, *14*, 477 – 480.
[36] R. G. Pearson, *Proc. Natl. Acad. Sci. USA* **1986**, *83*, 8440 – 8441.
[37] G. Desimoni, P. P. Righetti, E. Selva, G. Tacconi, V. Riganti, M. Specchiarello, *Tetrahedron* **1977**, *33*, 2829 – 2836.
[38] S. J. Gho, *Bull. Korean Chem. Soc.* **2003**, *24*, 731 – 732, and references therein.
[39] D. L. Heyl, S. Fernandes, L. Khullar, J. Stephens, E. Blaney, H. Opang-Owusu, B. Stahelin, T. Pasko, J. Jacobs, D. Bailey, D. Brown, M. C. Milletti, *Bioorg. Med. Chem.* **2005**, *13*, 4262 – 4268.
[40] Z. Zhou, R. G. Parr, *J. Am. Chem. Soc.* **1990**, *112*, 5720 – 5725.
[41] W. J. Ehlhardt, W. J. Wheeler, A. P. Breau, S. H. Chay, G. M. Birch, *Drug Metab. Dispos.* **1993**, *21*, 162 – 170.
[42] F. G. Hayden, A. R. Tunkel, J. J. Treanor, R. F. Betts, S. Allerheiligen, J. Harris, *Antimicrob. Agents Chemother.* **1994**, *38*, 1178 – 1181.
[43] a) G. Stoychev, B. Kierdaszuk, D. Shugar, *Eur. J. Biochem.* **2002**, *269*, 4048 – 4057; b) E. Kulikowska, B. Kierdaszuk, D. Shugar, *Acta Biochim. Pol.* **2004**, *51*, 493 – 531.
[44] E. D. Raczyńska, M. Makowski, M. Szeląg, B. Kamińska, K. Zientara, *J. Mol. Structure (THEOCHEM)* **2010**, *947*, 83 – 91.

[45] J. A. Maurinš, R. A. Paegle, M. J. Līdaks, E. I. Kvasyuk, P. V. Kuzmichkin, I. A. Mikhailopulo, *Nucleosides Nucleotides* **1986**, *5*, 79 – 93.
[46] J. D. Stoeckler, J. B. Ryden, R. E. Parks, Jr., M.-Y. Chu, M.-I. Lim, W.-Y. Ren, R. S. Klein, *Cancer Res.* **1986**, *46*, 1774 – 1778.
[47] A. Bzowska, E. Kulikowska, N. E. Poopeiko, D. Shugar, *Eur. J. Biochem.* **1996**, *239*, 229 – 234.
[48] K. Temburnikar, K. Brace, K. L. Seley-Radtke, *J. Org. Chem.* **2013**, *78*, 7305 – 7311.
[49] K. W. Temburnikar, S. C. Zimmermann, N. T. Kim, C. R. Ross, C. Gelbmann, C. E. Salomon, G. M. Wilson, J. Balzarini, K. L. Seley-Radtke, *Bioorg. Med. Chem.* **2014**, *22*, 2113 – 2122.
[50] C. Thibaudeau, P. Acharya, J. Chattopadhyaya, *Stereoelectronic effects in nucleosides and nucleotides and their structural implications*, 2nd ed.„ Department of bioorganic chemistry, Uppsala University, Uppsala, **2005**, p. 166.
[51] H. M. Kalckar, *Biochim. Biophys. Acta* **1953**, *12*, 250 – 264.
[52] A. E. Nixon, J. L. Hunter, G. Bonifacio, J. Eccleston, M. R. Webb, *Anal. Biochem.* **1998**, *265*, 299 – 307.
[53] J. A. Montgomery, J. H. Thomas, *J. Org. Chem.* **1971**, *36*, 1962 – 1967.
[54] J. A. Kelley, J. S. Driscoll, J. J. McCormack, J. S. Roth, V. E. Marquez, *J. Med. Chem.* **1986**, *29*, 2351 – 2358.
[55] V. V. Mossine, C. L. Barnes, M. S. Feather, T. P. Mawhinney, *J. Am. Chem. Soc.* **2002**, *124*, 15178 – 15179.
[56] V. V. Mossine, T. P. Mawhinney, *Adv. Carbohydr. Chem. Biochem.* **2010**, *64*, 291 – 402.
[57] H. M. Kalckar, *J. Biol. Chem.* **1947**, *167*, 477 – 486.
[58] P. E. Plesner, H. Klenow, *Preparation of ribose-1-phosphate in Methods in Enzymology, Vol. 3* (Eds.: S. P. Colowick. N. O. Kaplan), Academic Press, New York, **1957**, pp. 181 – 182.
[59] J. He, F. Seela, *Nucleic Acids Res.* **2002**, *30*, 5485 – 5496.

Received: April 5, 2015
Published online on July 31, 2015